1987-12

A computerized investigation using the method of images to predict the sound field in a fluid wedge overlying a slow fluid hal-space

Kaswandi, Carolus

Monterey, California: U.S. Naval Postgraduate School

NAVAL POSTGRADUATE SCHOOL

Monterey, California

THESIS

A Computerized Investigation Using the Method of Images to Predict the Sound Field in a Fluid Wedge Overlying a Slow Fluid Half-Space

by

Carolus Kaswandi

December 1987

Thesis Advisor: A. B. Coppens
Thesis Advisor: J. V. Sanders

UNCLASSIFIED
SECURITY CLASSIFICATION OF THIS PAGE

REPORT DOCUMENTATION PAGE

1a REPORT SECURITY CLASSIFICATION: UNCLASSIFIED	1b RESTRICTIVE MARKINGS
2a SECURITY CLASSIFICATION AUTHORITY	3 DISTRIBUTION/AVAILABILITY OF REPORT: Approved for public release; distribution is unlimited.
2b DECLASSIFICATION DOWNGRADING SCHEDULE	
4 PERFORMING ORGANIZATION REPORT NUMBER(S)	5 MONITORING ORGANIZATION REPORT NUMBER(S)
6a NAME OF PERFORMING ORGANIZATION: Naval Postgraduate School; 6b OFFICE SYMBOL (If applicable): 61	7a NAME OF MONITORING ORGANIZATION: Naval Postgraduate School
6c ADDRESS (City, State, and ZIP Code): Monterey, CA 93943-5000	7b ADDRESS (City, State, and ZIP Code): Monterey, CA 93943-5000
8a NAME OF FUNDING SPONSORING ORGANIZATION; 8b OFFICE SYMBOL (If applicable)	9 PROCUREMENT INSTRUMENT IDENTIFICATION NUMBER
8c ADDRESS (City, State, and ZIP Code)	10 SOURCE OF FUNDING NUMBERS: PROGRAM ELEMENT NO; PROJECT NO; TASK NO; WORK UNIT ACCESSION NO.

11 TITLE (Include Security Classification) A COMPUTERIZED INVESTIGATION USING THE METHOD OF IMAGES TO PREDICT THE SOUND FIELD IN A FLUID WEDGE OVERLYING A SLOW FLUID HALF-SPACE. UNCLASSIFIED

12 PERSONAL AUTHOR(S)
KASWANDI, CAROLUS

13a TYPE OF REPORT	13b TIME COVERED	14 DATE OF REPORT (Year, Month, Day)	15 PAGE COUNT
MASTER'S THESIS	FROM ________ TO ________	1987 - DECEMBER	86

16 SUPPLEMENTARY NOTATION

17 COSATI CODES			18 SUBJECT TERMS (Continue on reverse if necessary and identify by block number)
FIELD	GROUP	SUB-GROUP	Method of images, shallow water acoustics, acoustic propagation

19 ABSTRACT (Continue on reverse if necessary and identify by block number)

Sound fields in wedge-shaped ocean layers, modeling conditions on the continental shelf, have been studied at the Naval Postgraduate School in the last few years using the method of images. These studies are carried further in the present work. This method is implemented in different environmental conditions. This thesis examines the influence of several parameters on the sound field for downslope propagation in a wedge-shaped fluid of speed of sound c_2 overlying a slow bottom of speed of sound c_1. On the basis of qualitative and semi-quantitative analysis of the behavior of the pressure-depth profile for various geometrical and physical parameters, we can conclude that:

1. A defined distance, the "characteristic distance" $X_o = \pi/(2k_2 \sin\theta_o \tan\beta)$, where $\cos\theta_o = c_1/c_2$, $k_2 = \omega/c_2$, and β is the vertex angle of the wedge, has physical meaning as a useful scaling distance.

20 DISTRIBUTION/AVAILABILITY OF ABSTRACT: ☒ UNCLASSIFIED/UNLIMITED ☐ SAME AS RPT ☐ DTIC USERS	21 ABSTRACT SECURITY CLASSIFICATION: UNCLASSIFIED
22a NAME OF RESPONSIBLE INDIVIDUAL: A. B. COPPENS	22b TELEPHONE (Include Area Code): 646-2941; 22c OFFICE SYMBOL: 61

DD FORM 1473, 84 MAR — 83 APR edition may be used until exhausted. All other editions are obsolete.

SECURITY CLASSIFICATION OF THIS PAGE

☆ U.S. Government Printing Office: 1986—606-24.

UNCLASSIFIED

2. The distance of the source from the apex, in terms of the X_o, plays a major role in determining the downslope sound field.

Approved for public release, distribution is unlimited.

A Computerized Investigation Using the Method of Images to Predict the Sound Field in a Fluid Wedge Overlying a Slow Fluid Half-Space

by

Carolus Kaswandi
Commander, Indonesian Navy
B.S., Indonesian Navy Electronics School, 1967
Eng., Indonesian Navy Institute of Science, 1979

Submitted in partial fulfillment of the requirements for the degree of

MASTER OF SCIENCE IN PHYSICS

from the

NAVAL POSTGRADUATE SCHOOL
December 1987

ABSTRACT

Sound fields in wedge-shaped ocean layers, modeling conditions on the continental shelf, have been studied at the Naval Postgraduate School in the last few years using the method of images. These studies are carried further in the present work. The method is implemented in different environmental conditions. This thesis examines the influence of several parameters on the sound field for downslope propagation in a wedge-shaped fluid of speed of sound c_2 overlying a slow bottom of speed of sound c_1. On the basis of qualitative and semi-quantitative analysis of the behavior of the pressure-depth profile for various geometrical and physical parameters, we can conclude that:

1. A defined distance, the "characteristic distance" $X_o = \pi/(2k_2 \sin\theta_o \tan\beta)$, where $\cos\theta_o = c_1/c_2$, $k_2 = \omega/c_2$, and β is the vertex angle of the wedge, has physical meaning as a useful scaling distance.
2. The distance of the source from the apex, in terms of the X_o, plays a major role in determining the downslope sound field.

TABLE OF CONTENTS

LIST OF TABLES

LIST OF FIGURES

ACKNOWLEDGEMENTS

I would like to acknowledge Professor Alan B. Coppens who assigned this interesting topic. My thanks to Commander Chil Ki Baek who assisted Professor Alan B. Coppens thus making this job much easier. I thank my wife Tuti and my children, Henry, Anna, and Michael, for their patience and support. I thank those people in the Physics Department of the Naval Postgraduatre School who encouraged me to persevere.

Finally, I hope that in the future this work will be useful to others by expanding their knowledge in this field.

I. INTRODUCTION

A. SOUND PROPAGATION IN SHALLOW WATER CHANNEL

Experimental investigations of sound propagation in shallow water channels have been done by several investigators. Shallow water propagation is of interest because of the applications to coastal defense. These investigations are expensive and time consuming. The use of a computer model should provide a relatively inexpensive alternative to observation.

One of the techniques uses normal mode theory. The normal mode theory, which was introduced and developed by C. L. Perkeris [Ref. 1], gave the exact solution in water of constant depth. Further development of normal mode theory was made by L. Brekovskikh [Ref. 2], who initiated pressure as an integral involving Bessel functions and solution of the normal mode equation. Another theoretical approach to sound propagation in a horizontally stratified ocean of constant depth is given by the method of multiple scattering [Ref. 1]. With this method, all the previous theories can be simplified by conversion into an asymptotic form which is valid when the acoustic wavelength is small compared to the distance over which the sound speed varies appreciably. These theories agree with the laboratory experiments.

For a water channel with a small bottom slope, the sound field may be expressed approximately in terms of adiabatic normal modes. To facilitate prediction, R.D. Groves, Anton Nagl, H. Uberall, and G. L. Zauer [Ref. 3] modeled a wedge-shaped isovelocity ocean with a linearly-sloping, perfectly-rigid ocean floor using adiabatic normal modes. For a penetrable bottom the normal mode description fails when modes propagating upslope encounter the "critical depth" (H_c), defined as the depth where the associate mode changes from fully trapped within the water channel to radiating energy into the bottom (cut off) [Ref. 4-6]. The parabolic equation can be used to explain the mechanism of sound energy radiation into the bottom [Ref. 7,8]. Such an equation was studied by F. B. Jensen and W. A. Kuperman [Ref. 9], with predictions that satisfactorily agreed with the experimental results for small ray angles. With some restrictions, normal mode theory is applicable for sound propagation in the wedge-shaped fluid with a fast bottom. The parabolic equation is good for fast and slow bottom, but with the restriction that horizontal ray angles must be less than 20°.

Another technique introduced to predict the propagation of sound in the wedge is the method of images. This method was derived from the simplest case; a monofrequency point source in a homogeneous ocean with parallel boundaries. The total pressure is the sum of an infinite number of spherical waves from an infinite set of images. The restriction of this method is that it does not generalize to the case of inhomogeneous media or non-planar boundaries. In this work, this method will be studied.

B. THE METHOD OF IMAGES

In 1978, Coppens, Sanders, Ioannou, and Kawamura [Ref. 10], predicted the pressure amplitude and phase of the sound field along the bottom of a wedge-shaped fluid layer of density ρ_1, and speed of sound c_1, overlying a fast fluid bottom of density ρ_2, and speed of sound $c_2 > c_1$ by applying the method of images in a computer program implementation. In 1984, Baek [Ref. 11], and LeSesne [Ref. 12], implemented further improvements. Baek's computer program, WEDGE, and LeSesne's computer program XSLOPE were validated for several cases. WEDGE was developed for two-dimensional upslope propagation (the source and received are in the same vertical plane perpendicular to the shore line, and the receiver is closer to the apex than the source (Figure 1.1a)) and downslope propagation (the source is closer to the apex than the receiver (Figure 1.1b)). XSLOPE was developed for upslope, downslope, or cross-slope propagation (the source, receiver, and apex, are not necessarily in the same plane perpendicular to the shore line (Figure 1.1c)). In both programs, Baek and LaSesne assume that the fluid in the wedge and fluid in the bottom have constant densities, that the speed of sound is constant, and that the interface between the fluids and the surface is smooth.

In both WEDGE and XSLOPE, all distances are scaled in units of the "dump distance." A dump distance X, as stated in Reference 10, is the distance from the apex measured along the interface at which the lowest mode attains cutoff. If the wedge angle is β (Figure 1.1c), then

$$X = \frac{\pi/2}{k_1 \sin\theta_c \tan\beta} \tag{1.1}$$

$$\theta_c = \arccos(c_1/c_2) \tag{1.2}$$

where k_1 is the wave number in the wedge and θ_c is the critical grazing angle for reflection of sound from the bottom. For $\beta < < 1$

$$X = H \tan \beta \tag{1.3}$$

This scaling distance negates the necessity of specifying frequency.

C. COMPUTER PROGRAM DSLOW

At the start of the work reported in this thesis, a computer program was obtained [Ref. 13], which is an extension of the WEDGE and XSLOPE for downslope configuration with a slow bottom. The computer model, DSLOW, developed to run on a desktop computer (Wang 2000), uses the method of images to predict the pressure amplitude and phase anywhere within the wedge fluid overlying a slow bottom in a cross-slope configuration. A geometrical picture of this configuration is shown in Figure 1.1c.

Mathematically, the model used in WEDGE and XSLOPE is applicable in any condition. But consideration must be given for making it work for a slow bottom. In the case of a fast bottom, the dump distance has a physical meaning. The dump distance is expressed as a function of the critical angle. The critical angle is equal to arccos (c_1/c_2). In the case of slow bottom, c_1/c_2 is greater than 1, thus arccos (c_1/c_2) is invalid; therefore, so is the dump distance. To facilitate the scaling factor, a "characteristic distance" or "scaling distance" is introduced. We need the scaling distance because, with this distance, our model will be independent of frequency as in the fast bottom case. There is also the hope that the use of a scaling distance will allow systematic observation of the pressure field. This scale distance X_o is the distance measured along the interface from the apex to the point where the lowest mode would attain cutoff if the fluids in the wedge and in the bottom were to be interchanged. The characteristic distance is defined by the following equation:

$$X_o = \frac{\pi/2}{k_2 \sin\theta_o \tan\beta} \qquad (1.4)$$

where $\theta o = \arccos(c_2/c_1)$ and $K_2 = \omega/c_2$ is the wave number in the bottom.

The following terms will be used throughout (see Figure 1.1):

β = wedge angle

R_1 = distance of the source from the apex in units of X_o

R_2 = distance of the receiver from the apex in units of X_o

γ = angle of elevation of the source above the bottom

δ = angle of elevation of the receiver above the bottom

Y_o = distance between the projection of the source and receiver on the shore line, scaled by X_o

ρ_1/ρ_2 is the ratio between the density of the fluid in the wedge (ρ_1) and the density of the fluid in the bottom (ρ_2)

c_1/c_2 is the ratio between the speed of sound in the wedge (c_1) and the speed of sound in the bottom (c_2). A fast bottom occurs when $c_2 > c_1$; a slow bottom occurs when $c_2 < c_1$

The purpose of this research is the following:

1. To transfer, test, and evaluate DSLOW program on the IBM 3300;
2. To obtain numerical and graphical output for a number of cases; and
3. To attempt to develop plausible explanations for any significant features observed.

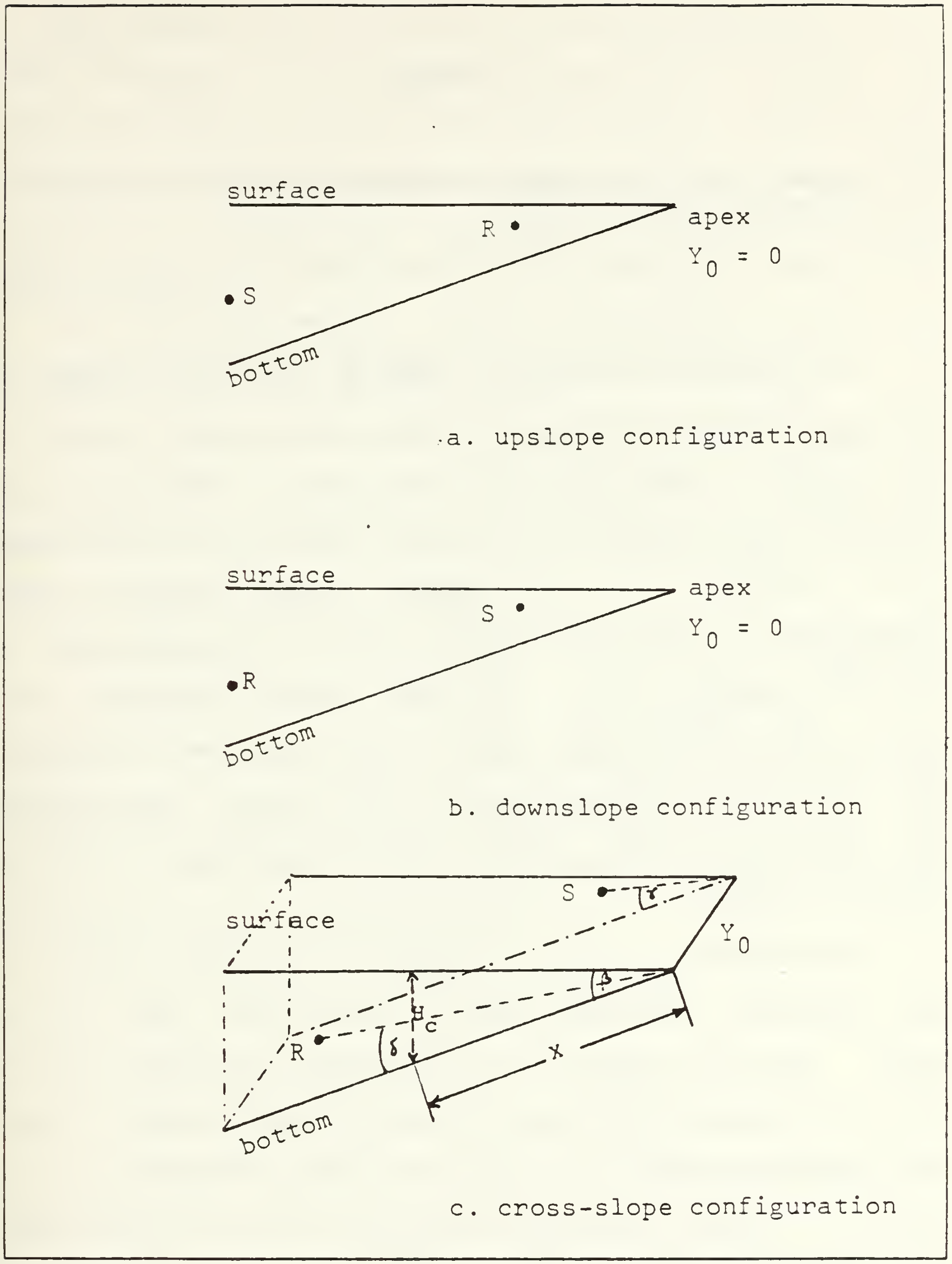

Figure 1.1 Geometry of the wedge

II. THEORY

A. GENERAL VIEW OF A WEDGE PRESSURE DISTRIBUTION IN THE DOWNSLOPE CONFIGURATION

A general picture of the sound energy propagation within the wedge in downslope direction is given in Figure 2.1. If a sound source is placed at point S, ray 1 will reach the surface at point P with an incident angle α with respect to the normal to the surface at this point. This ray is reflected by the surface at the same angle but with the phase 180° different. (On the surface, sound pressure is zero everywhere.) The reflected ray reaches the bottom with an incident angle $\beta + \alpha$. At great enough distance, ray 1 never reaches the bottom again. This ray does not contribute to a sound pressure field at the bottom. The pressure at the bottom should be very small according to the ray theory argument.

Using these ray-tracing methods, an estimated profile of the pressure amplitude versus the receiver depth can be made. When the source and the receiver are placed near the apex, the pressure amplitude is zero at the surface, a maximum somewhere within the wedge, and greater than zero at the bottom. In the case where the source is at a far distance, the pressure amplitude is equal to zero at the surface, a maximum somewhere within the wedge, and zero at the bottom.

Ray tracing will only give a rough approximation, not an exact solution, but ray tracing may be used as a guide. The method of images calculates the exact pressure amplitude at each point within the wedge subject only to the assumption inherent in using the plane-wave Rayleigh reflection coefficients.

B. SOUND PRESSURE AT A POINT IN THE WEDGE DOWNSLOPE PREDICTED BY THE METHOD OF IMAGES

Let the source be a scaled distance R_1 from the apex and at an angle of γ measured from the bottom of the wedge. Let the receiver be a scaled distance R_2 from the apex and at an angle δ measured from the bottom.

Using Figure 2.2, let the upper half family of images be $n = 1,2,3,4,...$ and the lower half family be $n' = 1,2,3,4....$ Calculating the field resulting from source and images proceeds along the lines developed in [Ref. 14]. If ϕ_n is the angle formed at the apex between the n_{th} image of the source and the receiver, then

$$\phi_1 = 2\beta - \delta - \gamma$$

$$\phi_2 = 2\beta - \delta + \gamma$$

$$\phi_3 = 4\beta - \delta - \gamma$$

$$\phi_4 = 4\beta - \delta + \gamma$$

....

....

....

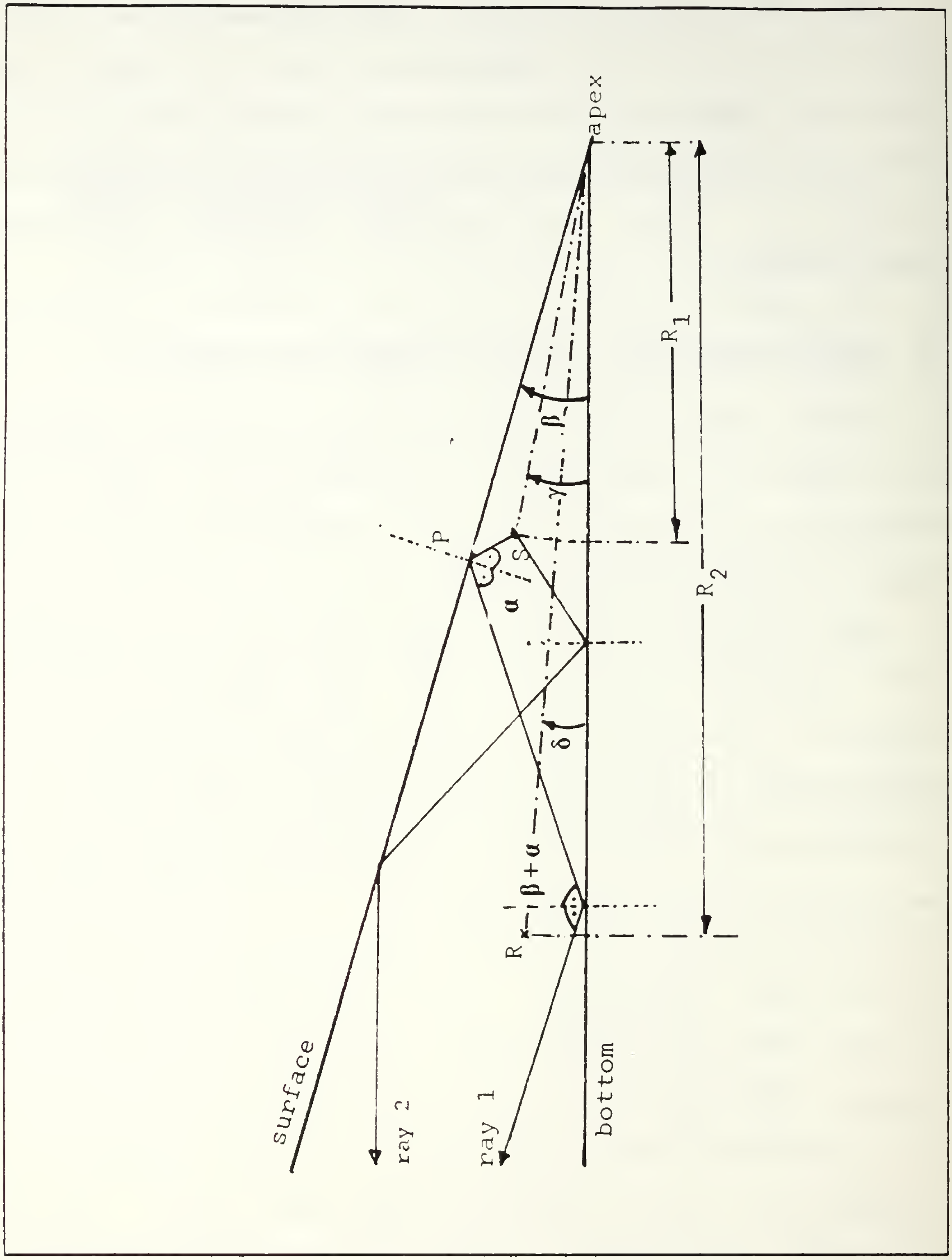

Figure 2.1 Ray tracing in the wedge downslope

or more generally

$$\phi_n = (n + 1)\beta - \delta - \gamma \qquad \text{for } n \text{ odd}$$

$$\phi_n = n\beta - \delta + \gamma \qquad \text{for } n \text{ even}$$

Which can be reduced to:

$$\phi_n = \{n+(1/2)[1-(-1)^n]\}\beta + (-1)^n\gamma - \delta \qquad (2.1)$$

or

$$\phi_n = 2\ \mathrm{INT}\left[\frac{n + 1}{2}\right]\beta + (-1)^n\gamma - \delta \qquad (2.2)$$

where INT[ ] denotes the largest integer which is equal to, or smaller than the argument. Using the same method for the member n' of the lower family of images we obtain:

$$\phi_{n'} = \{n+(1/2)[1-(-1)^n]\}\beta + (-1)^n\gamma + \delta \qquad (2.3)$$

or

$$\phi_{n'} = 2\ \mathrm{INT}\left[\frac{n + 1}{2}\right]\beta + (-1)^n\gamma + \delta \qquad (2.4)$$

Using the geometry of Figures 2.2 and 2.4, the distance between the n^{th} and n'^{th} images to the receiver is respectively

$$r_n = \sqrt{R_1^2 + R_2^2 - 2R_1R_2\cos\phi_n} \qquad (2.5)$$

and

$$r_{n'} = \sqrt{R_1^2 + R_2^2 - 2R_1R_2\cos\phi_n} \qquad (2.6)$$

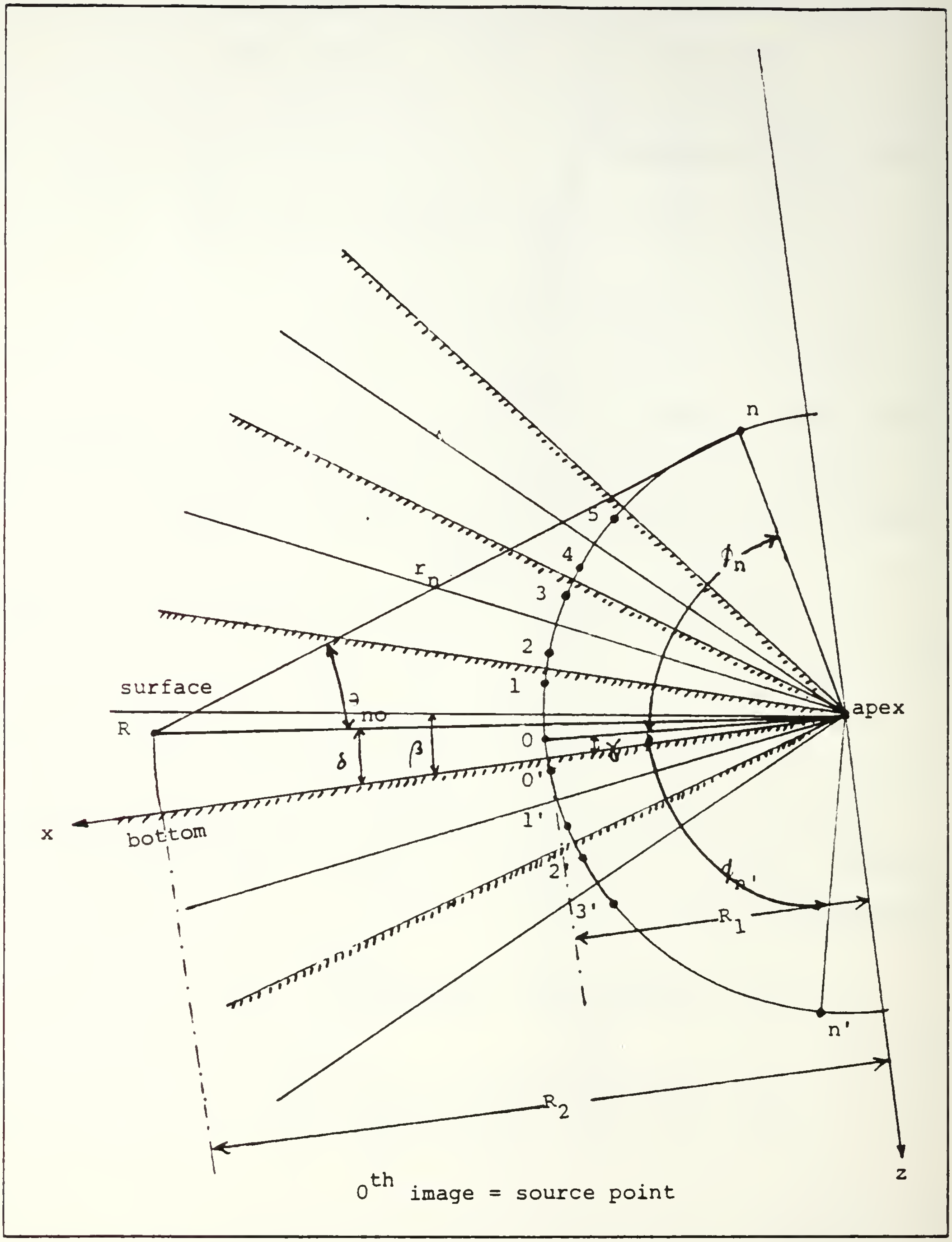

Figure 2.2 Geometry of a wedge by the method of images

The angles θ_{no} and $\theta_{n'o}$ for the n^{th} and n'^{th} images respectively are

$$\theta_{no} = \arc \tan \left[\frac{\sin \phi_n}{R_2/R_1 - \cos \phi_n} \right] \tag{2.7}$$

and

$$\theta_{n'o} = \arc \tan \left[\frac{\sin \phi_{n'}}{R_2/R_1 - \cos \phi_{n'}} \right] \tag{2.8}$$

Define θ_{nm} and $\theta_{n'm}$ as the angles of incidence for the m^{th} bounces from the bottom for the n and n' image respectively; m = 1,2,3.... (The 0^{th} bounce is the last one before reaching the receiver.) The geometry of Figures 2.2 and 2.3 give θ_{nm} as follows:

$$\theta_{21} = \theta_{20} - 2\beta - \delta$$

$$\theta_{32} = \theta_{30} - 4\beta - \delta$$

$$\theta_{41} = \theta_{40} - 2\beta - \delta$$

$$\theta_{52} = \theta_{50} - 4\beta - \delta$$

....

....

....

The general expression is

$$\theta_{nm} = \theta_{no} - 2m\beta - \delta$$

Using the same method

$$\theta_{n'm} = \theta_{n'o} - 2m\beta + \delta$$

The maximum number of bottom bounces of the n^{th} and n'^{th} image is

$$m_{max} = M = \text{INT}\ [\phi_n/2\beta] = \text{INT}\ [\phi_{n'}/2\beta]$$

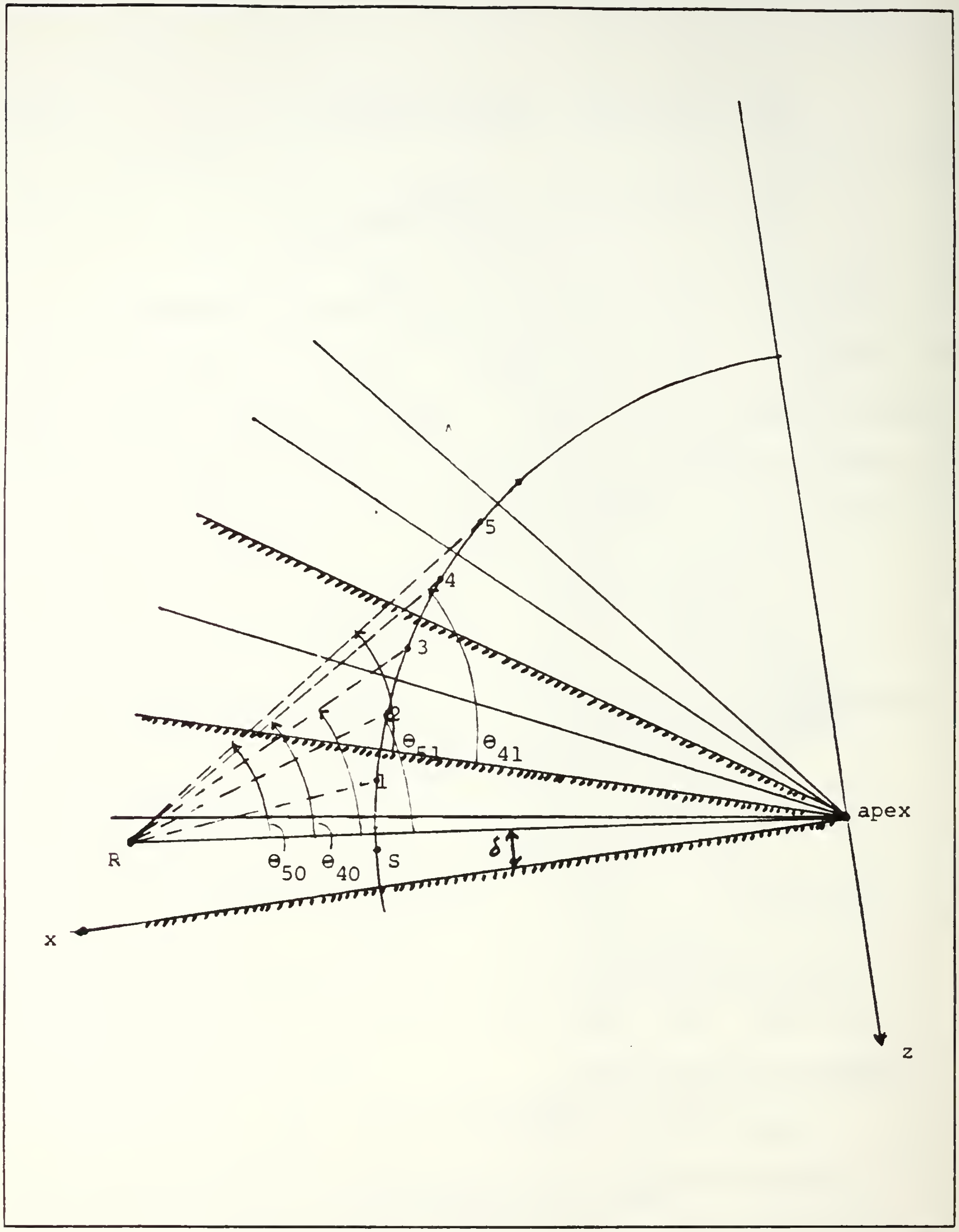

Figure 2.3 Geometric development of reflection angles

The maximum number of images is

$$n_{max} = N = \text{INT}\ [\pi/\beta]$$

The reflection coefficients for the n^{th} and n'^{th} images for a plane wave are:

$$R(\theta_{nm}) = \frac{\frac{\rho_1 c_1}{\rho_2 c_2} - \psi_{nm}}{\frac{\rho_1 c_1}{\rho_2 c_2} + \psi_{nm}} \qquad (2.9)$$

and

$$R(\theta_{n'm}) = \frac{\frac{\rho_1 c_1}{\rho_2 c_2} - \psi_{n'm}}{\frac{\rho_1 c_1}{\rho_2 c_2} + \psi_{n'm}} \qquad (2.10)$$

where

$$\psi_{nm} = \frac{\sqrt{1 - (c_1/c_2)^2 \cos^2 \theta_{nm}}}{\sin \theta_{nm}} \qquad (2.11)$$

and

$$\psi_{n'm} = \frac{\sqrt{1 - (c_1/c_2)^2 \cos^2 \theta_{n'm}}}{\sin \theta_{n'm}} \qquad (2.12)$$

The contribution from the upper family of images is

$$Pu = \sum_{n=1}^{N} \frac{1}{r_n} \exp(-jkr_n)(-1)^{\text{INT}[n+1)/2]} \prod_{m=0}^{M} R_{nm} \qquad (2.13)$$

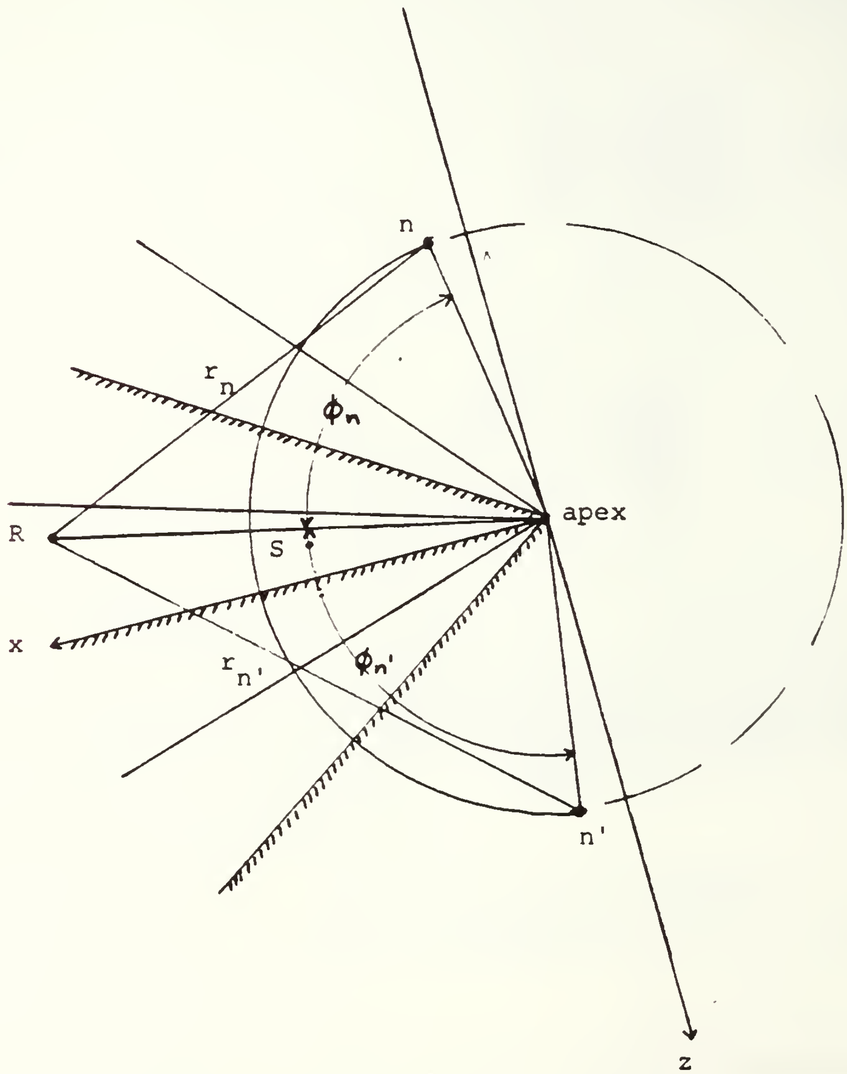

Figure 2.4 Geometry of symmetric images

and for lower family of images is

$$Pu = \sum_{n=1}^{N} \frac{1}{r_{n'}} \exp(-jkr_{n'})(-1)^{INT[n+1)/2]} \prod_{m=0}^{M} R_{n'm} \qquad (2.14)$$

The total complex pressure is

$$P(x) = Pu + Pl \qquad (2.15)$$

III. DSLOW PROGRAM IMPLEMENTATION

A. PROGRAMS FEATURES

Since the mainframe graphics computer was available, the DISSPLA graphical program was used. The only programming language compatible with DISSPLA is FORTRAN. The numerical and graphical output is provided by this program. To give the pressure amplitude versus received angle graphs, two-dimensional plotting is used.

The program DSLOW is run by placing the point source anywhere in the wedge and then placing the receiver at a distance downslope from the source. The receiver position was varied from zero degrees at the bottom to β at the surface. High resolution plotting was achieved by dividing the y-axis (received angle) into two regions. The first region covers the receiver angles from zero to 1/5 of the wedge angle. In this region $\Delta\delta$ is equal to $\beta/100$. The second region covers the remaining wedge angle with $\Delta\delta$ equal to $\beta/10$. This method provides 29 predictions of the pressure amplitude. Another method of plotting carried out was in the region of $\delta > \beta/2$, $\Delta\delta = \beta/10$, and in the region of $\delta < \beta/2$, $\Delta\delta = \beta/100$. This method provides 54 points to be plotted.

B. NORMALIZATION

The main goal of this research was to investigate the profile of the pressure amplitude as a function of a number of variables. An example of the numerical values of the pressure amplitude, the normalized pressure amplitude, and the phase at each receiver position is displayed in Appendix C. The sound pressure becomes smaller as the receiver is moved away from the source. If the pressure amplitude were plotted directly, it would be difficult to compare the curves at near distances to the curves at far distances since at the near distances the pressure amplitude is much greater than the pressure amplitude in far distance. Thus, a normalized pressure amplitude is needed. The normalized pressure is obtained as follows: (see Figure 3.1)

We know that the sound pressure at the surface is zero and that the sound pressure is a small number greater than zero at a point near the surface. The first non-zero value of pressure P_1 is at the receiver angle, $\delta_1 = 9\beta/10$. We use this first calculated non-zero pressure amplitude as the normalization unit. The normalized pressure is

$$PN = P(\delta)/(P_1) \tag{3.1}$$

where $P(\delta)$ is the pressure at any point within the wedge.

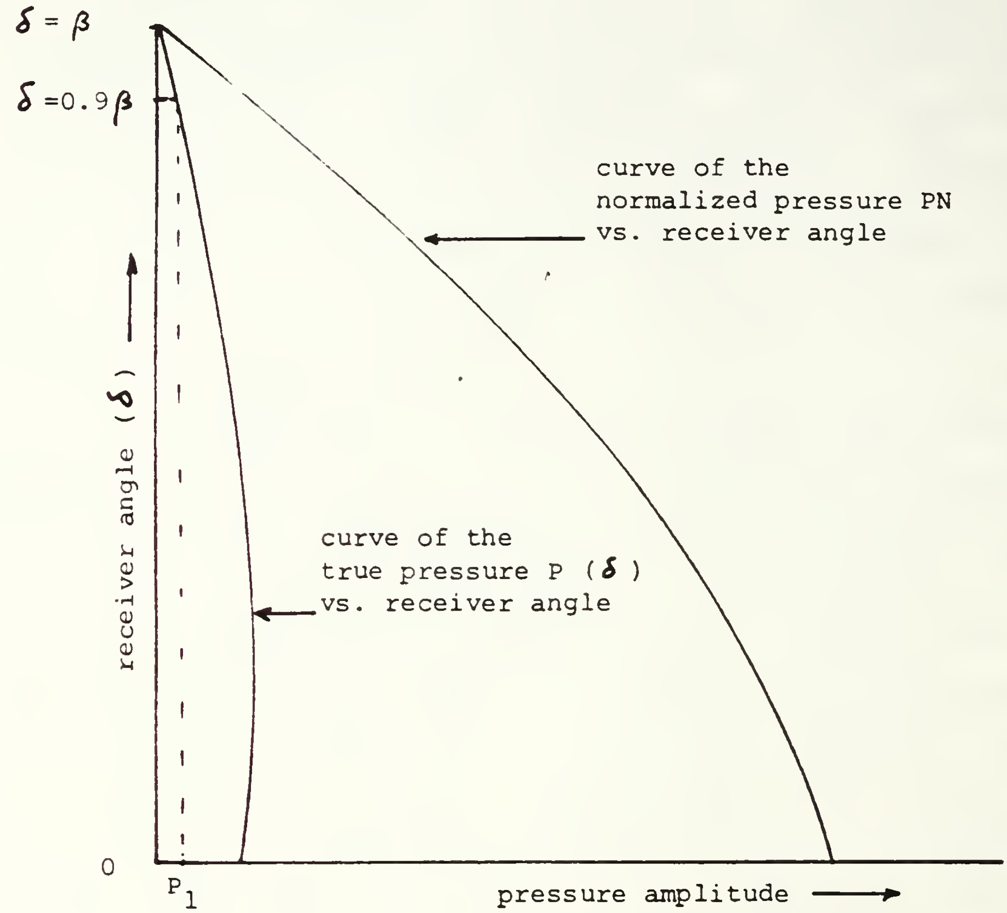

Figure 3.1 Pressure amplitude normalization

C. PROCEDURE

Figures 3.2 through 3.7 represent the results when the receiver distance and source angle are fixed and the source distance and receiver angle are varied. Figures 3.8 through 3.13 represent the results when the source distance and angle are fixed and the received distance and angle are varied. These cases will be the foundation of our subsequent discussions.

The solid lines indicate the fitted curve and the dots indicate some values of the normalized pressure amplitude. In DSLOW, the dot appears at each third datum.

D. PROGRAM IMPROVEMENT

DSLOW was designed to provide three-dimensional graphs. For example, the x-axis represents the scaled source distance, the y-axis represents the scaled received distance, and z-axis represents the normalized pressure amplitude. To simplify the presentation, only two-dimensional graphs were presented with the x-axis the normalized pressure amplitude and the y-axis the receiver angle δ. All curves are presented with the data fitted with a cubic spline.

The DSLOW program was executed to obtain numerical results of the phase angle, the pressure amplitude, and the normalized pressure amplitude at each receiver position. The first run used double precision for accuracy. Difficulties were encountered when the DISSPLA subprogram was attached for making the graphical output. When double precision and DISSPLA were not successful, the single precision was used, resulting in round-off error. (See Figure 3.8 at R_2 = 10.0.)

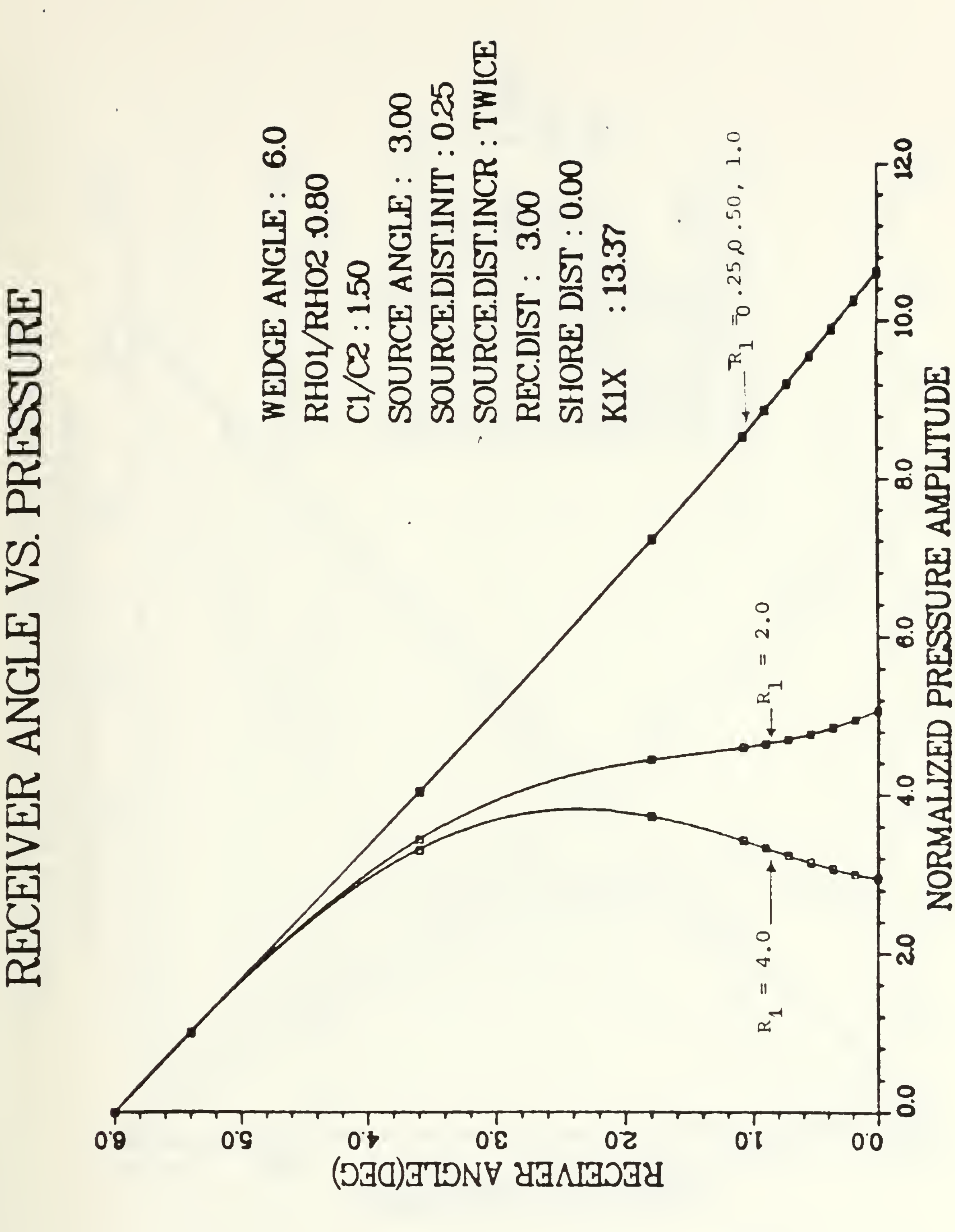

Figure 3.2 Graphs of receiver angle δ versus pressure amplitude with R_2 fixed, R_1 varied

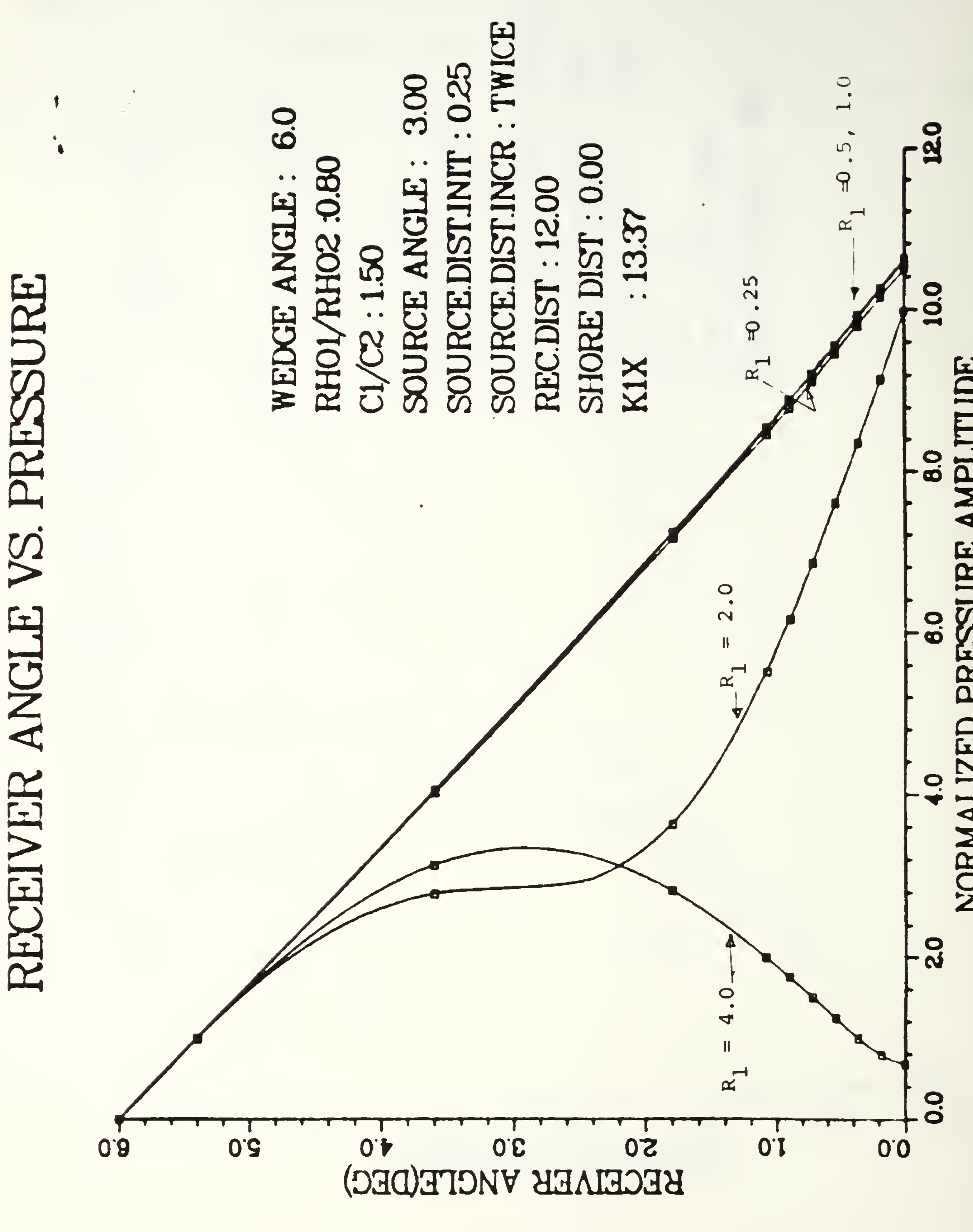

Figure 3.3 Graphs of receiver angle δ versus pressure amplitude with R_2 fixed, R_1 varied

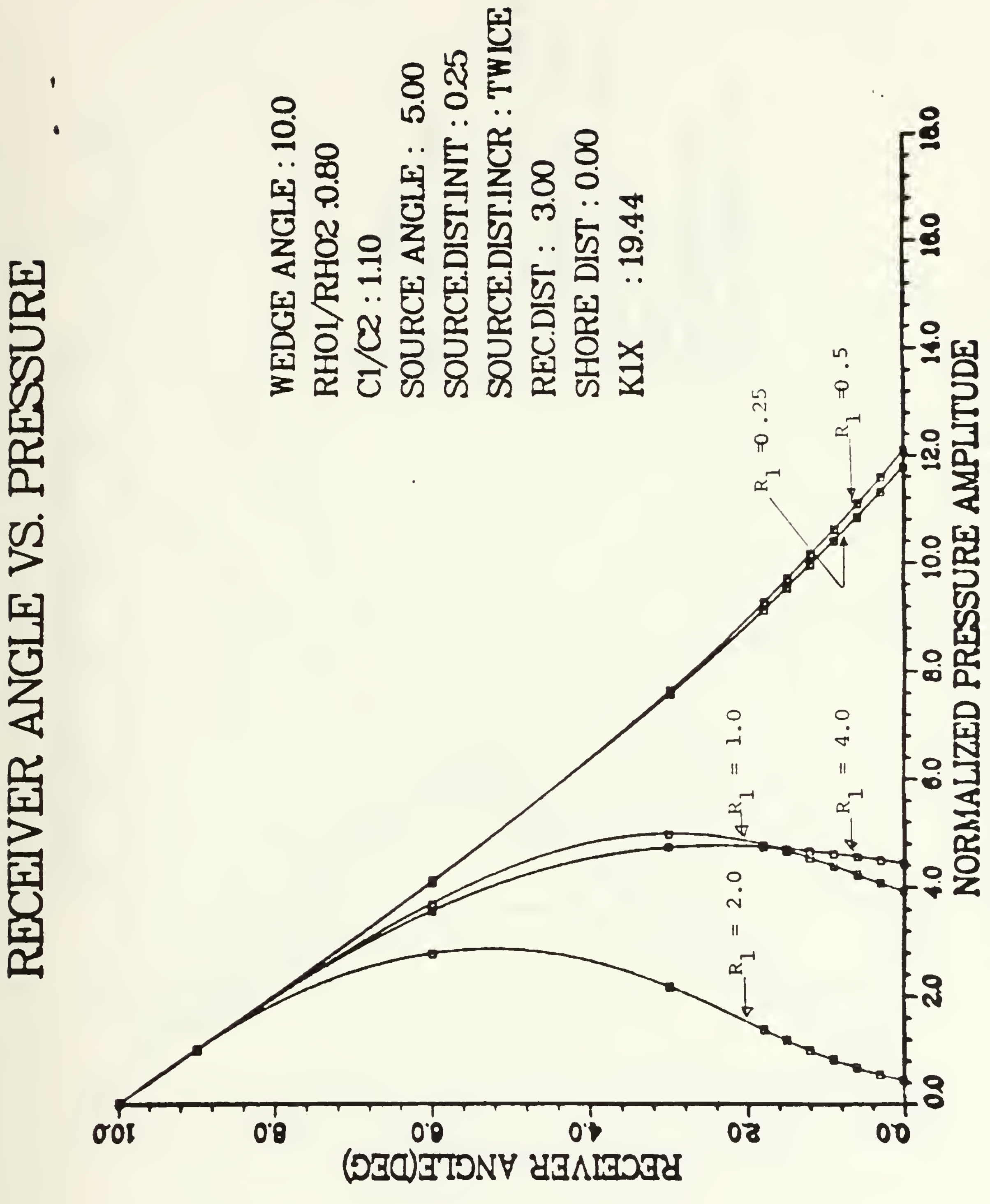

Figure 3.4 Graphs of receiver angle δ versus pressure amplitude with R_2 fixed, R_1 varied

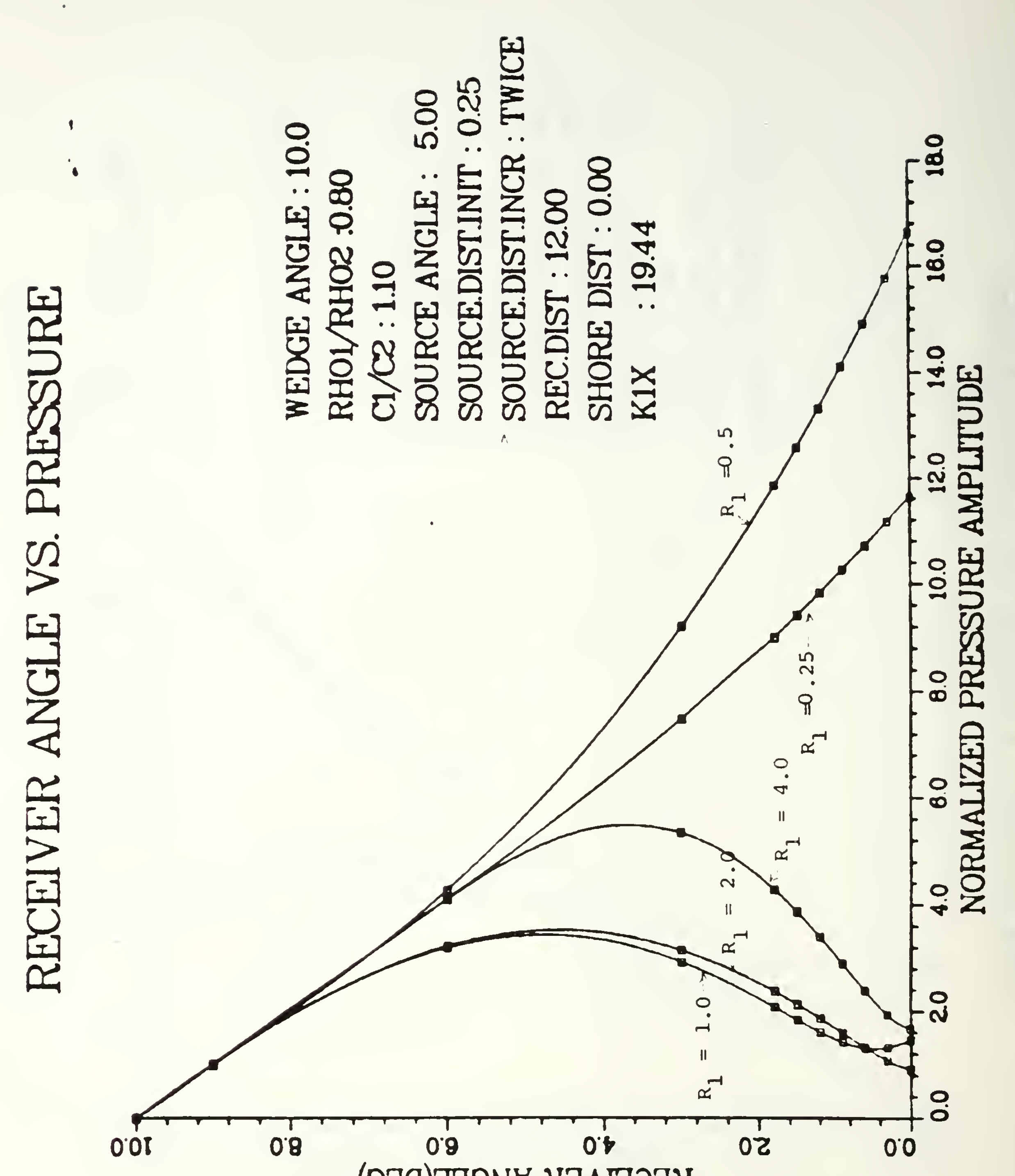

Figure 3.5 Graphs of receiver angle δ versus pressure amplitude with R_2 fixed, R_1 varied

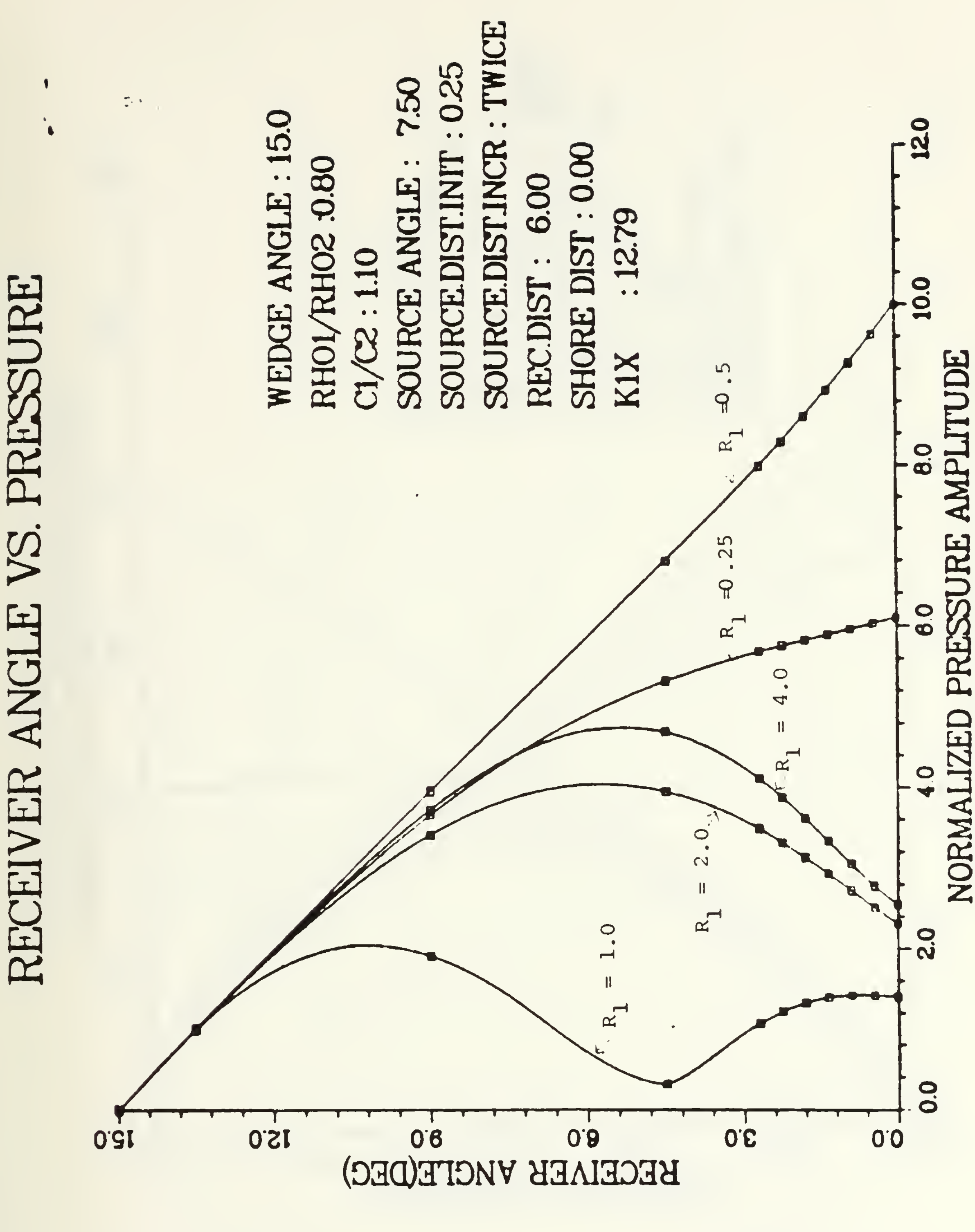

Figure 3.6 Graphs of receiver angle δ versus pressure amplitude with R_2 fixed, R_1 varied

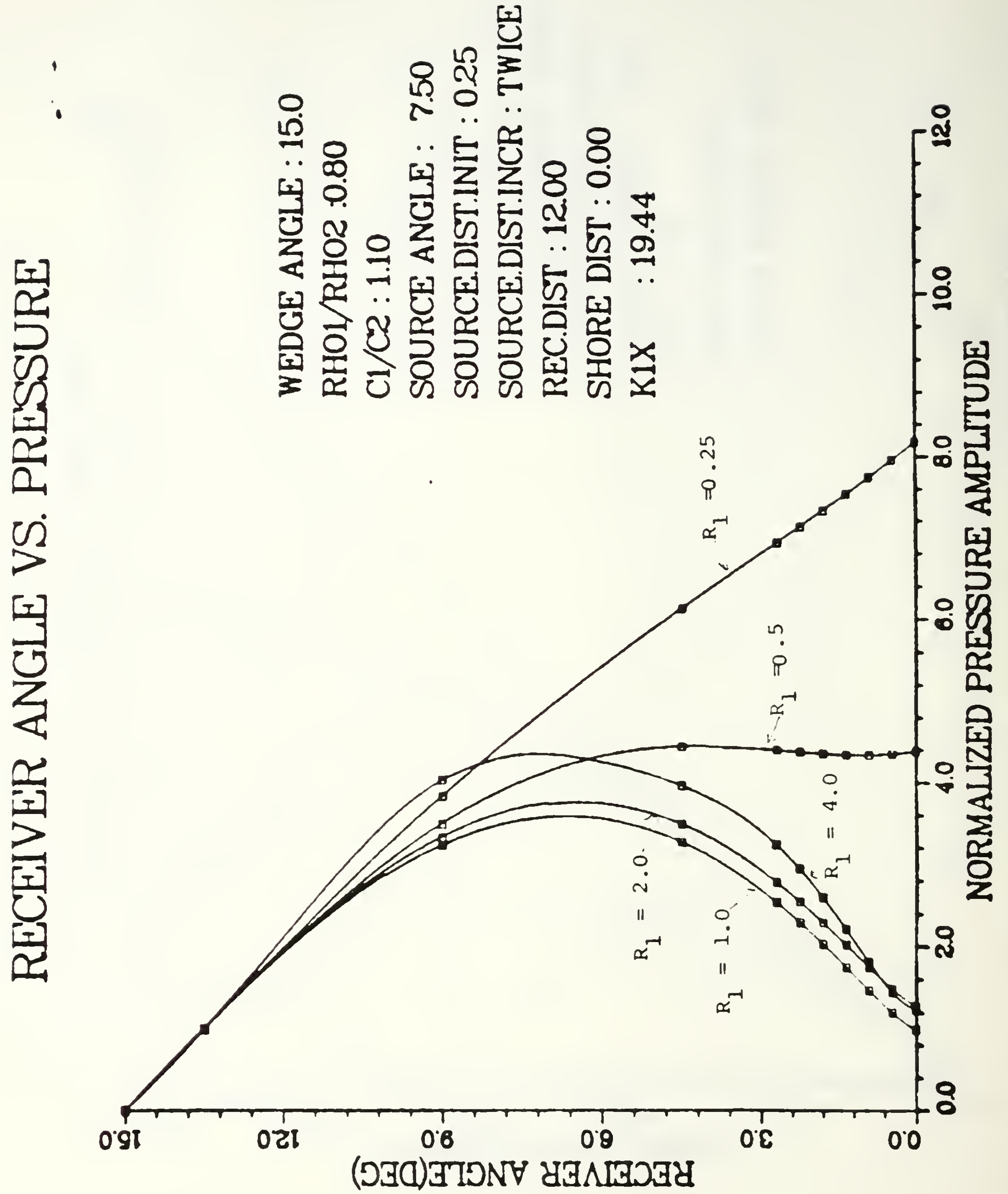

Figure 3.7 Graphs of receiver angle δ versus pressure amplitude with R_2 fixed, R_1 varied

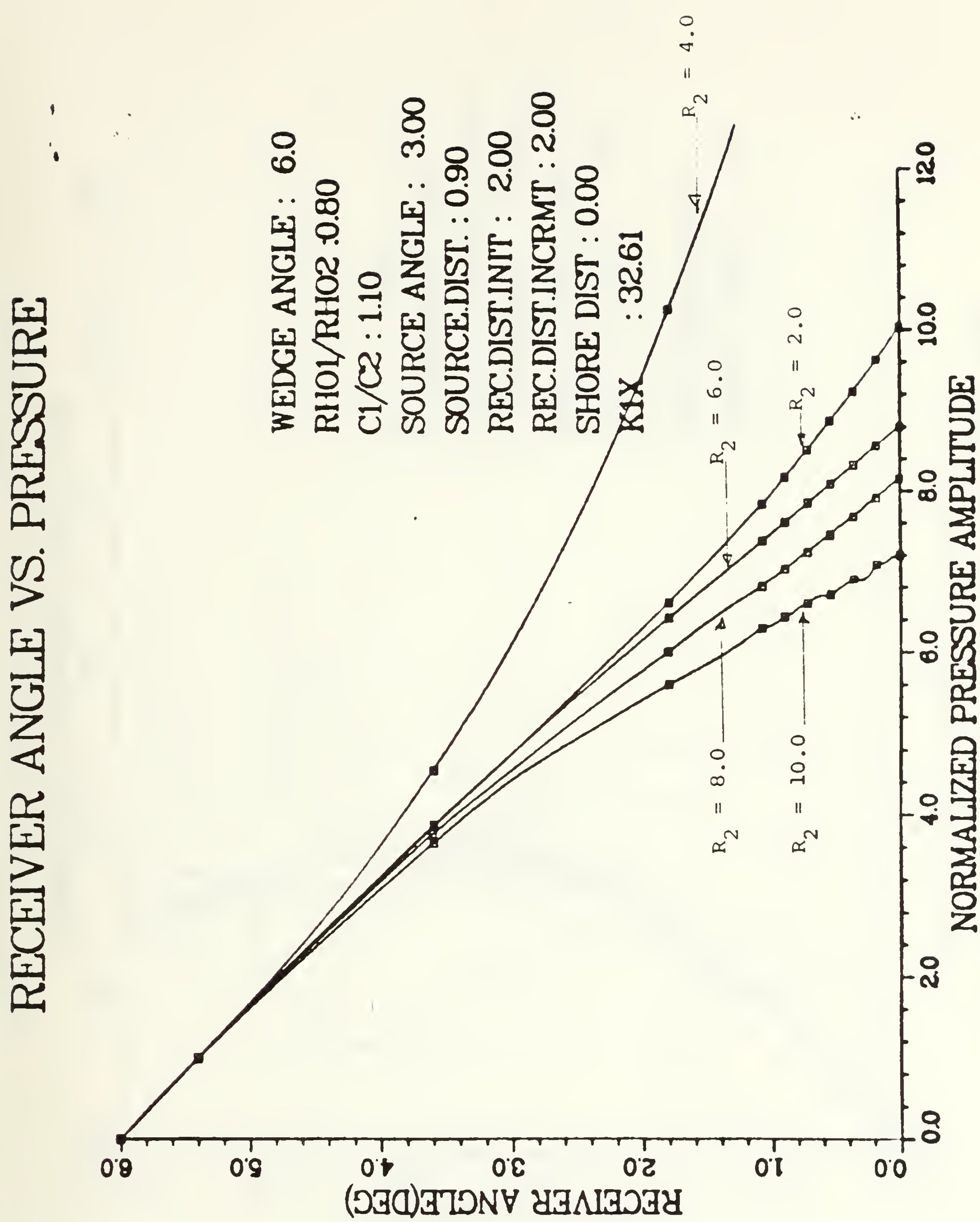

Figure 3.8 Graphs of receiver angle δ versus pressure amplitude with R_2 fixed, R_1 varied

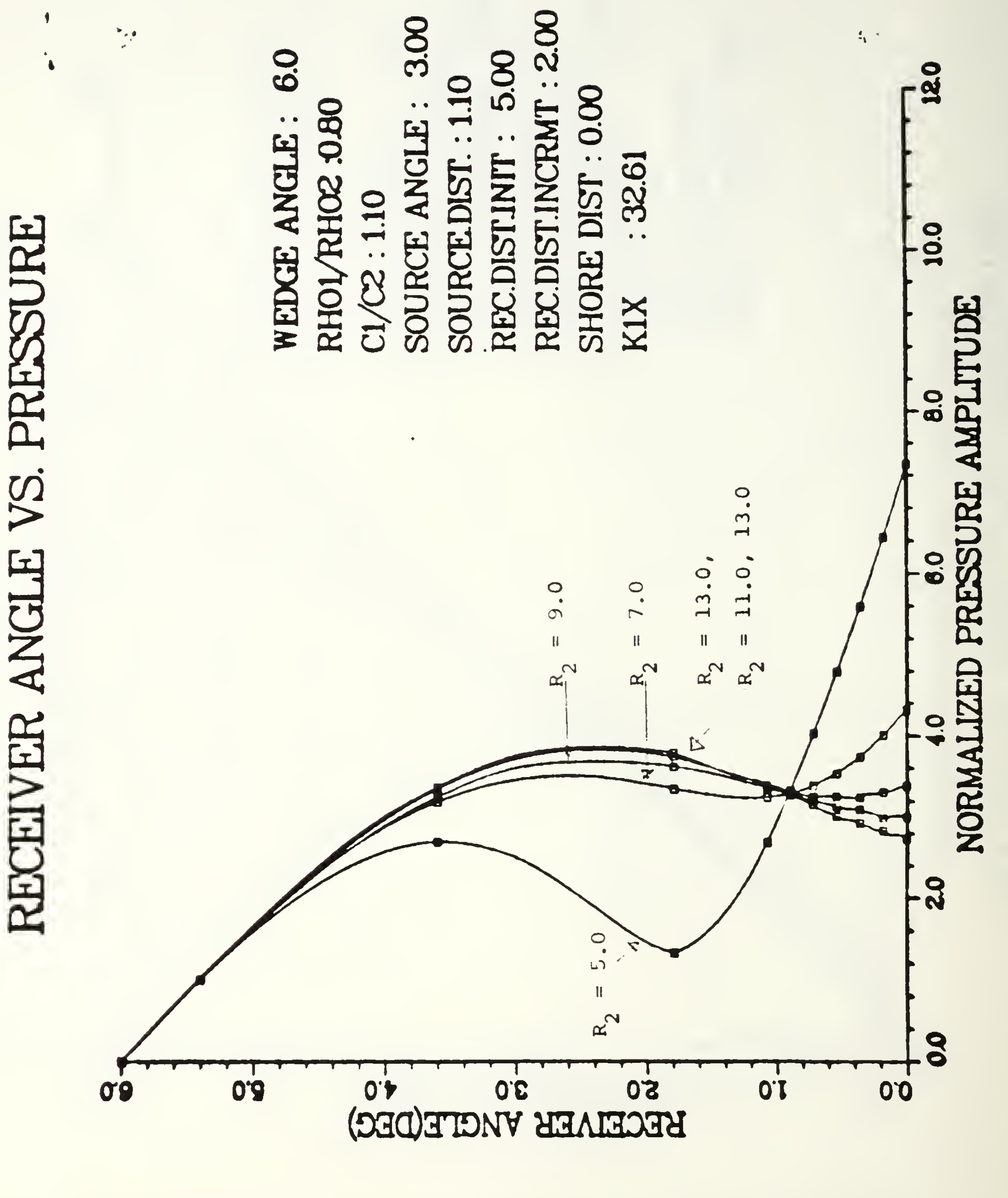

Figure 3.9 Graphs of receiver angle δ versus pressure amplitude with R_2 fixed, R_1 varied

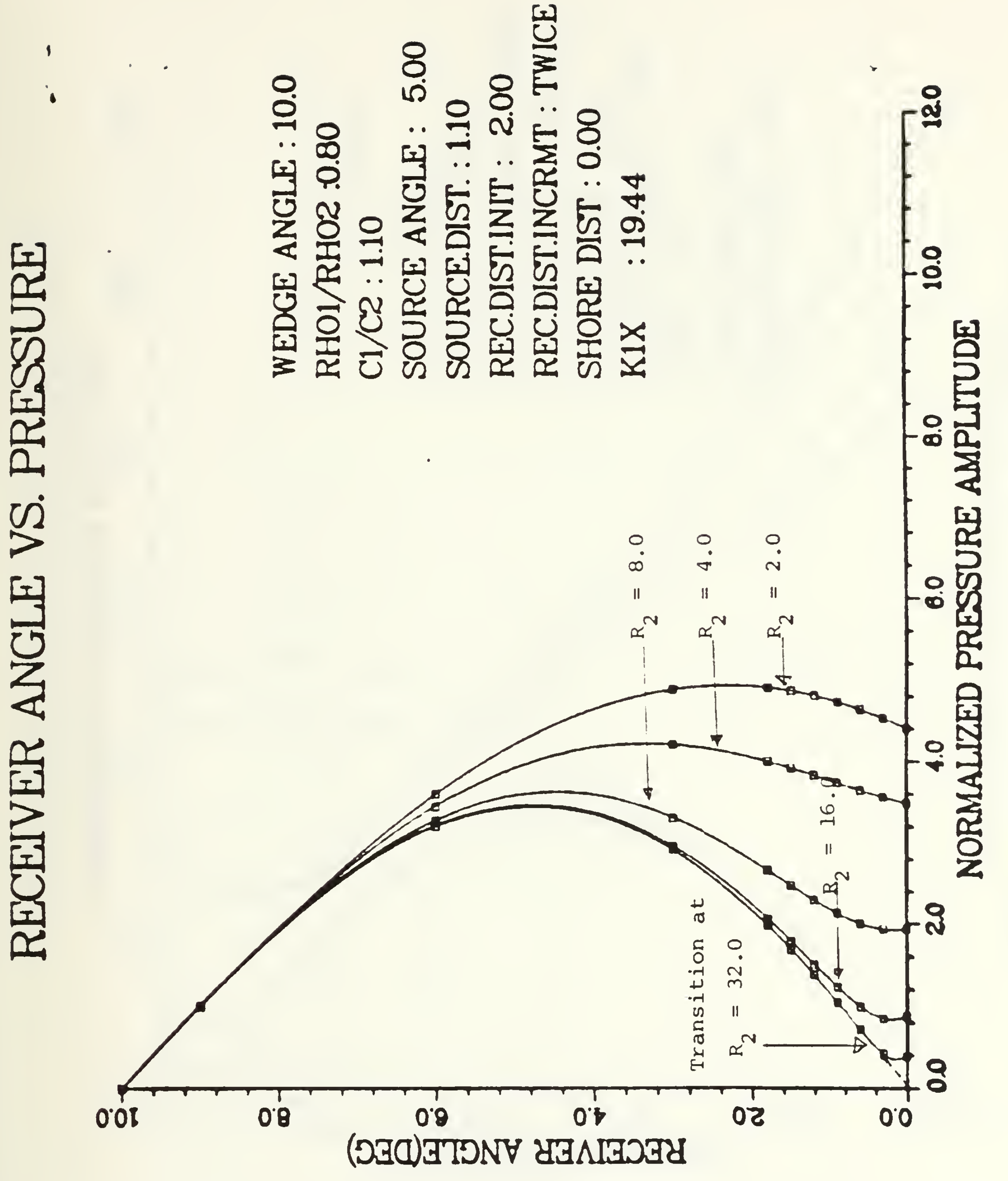

Figure 3.10 Graphs of receiver angle δ versus pressure amplitude with R_2 fixed, R_1 varied

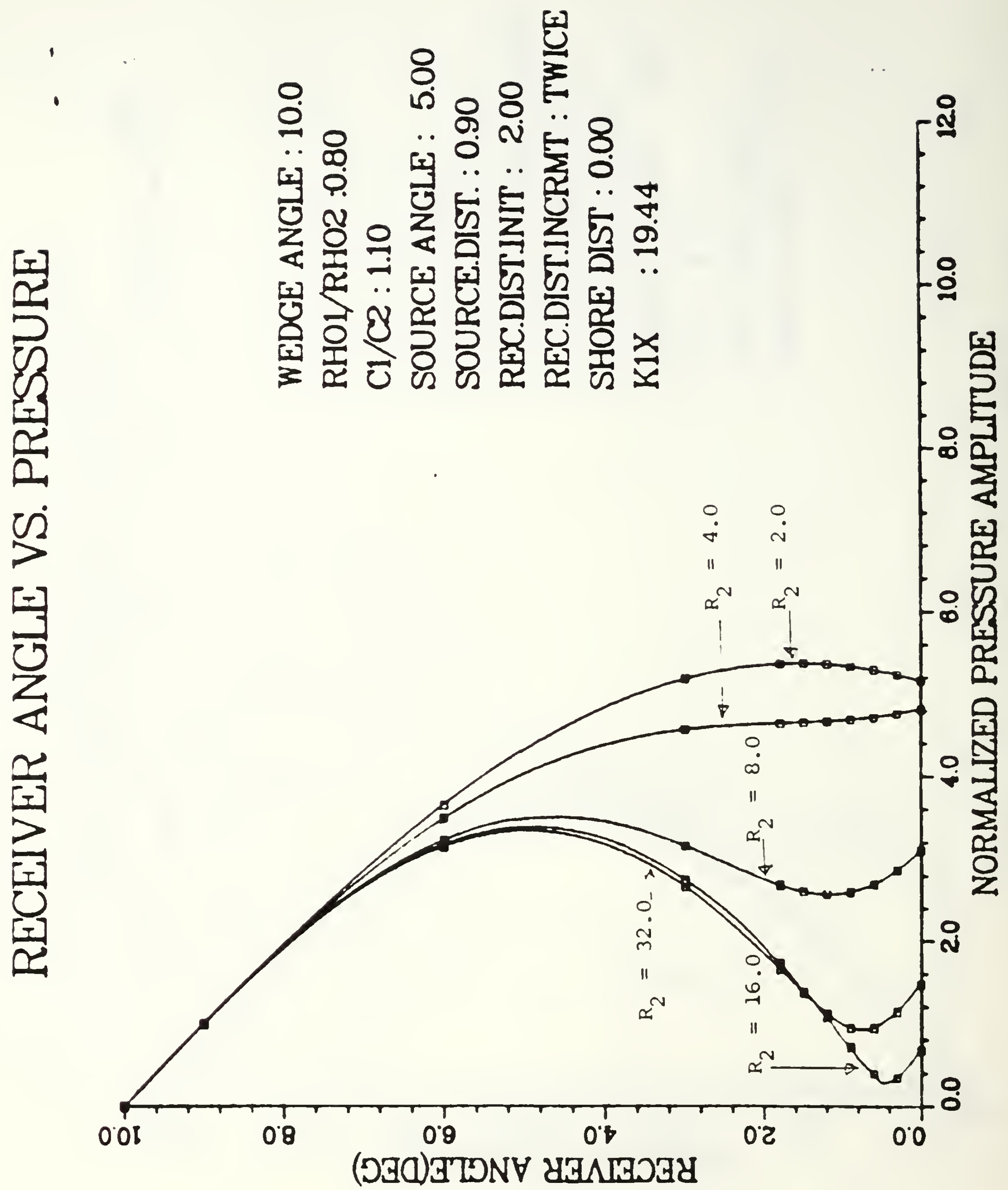

Figure 3.11 Graphs of receiver angle δ versus pressure amplitude with R_2 fixed, R_1 varied

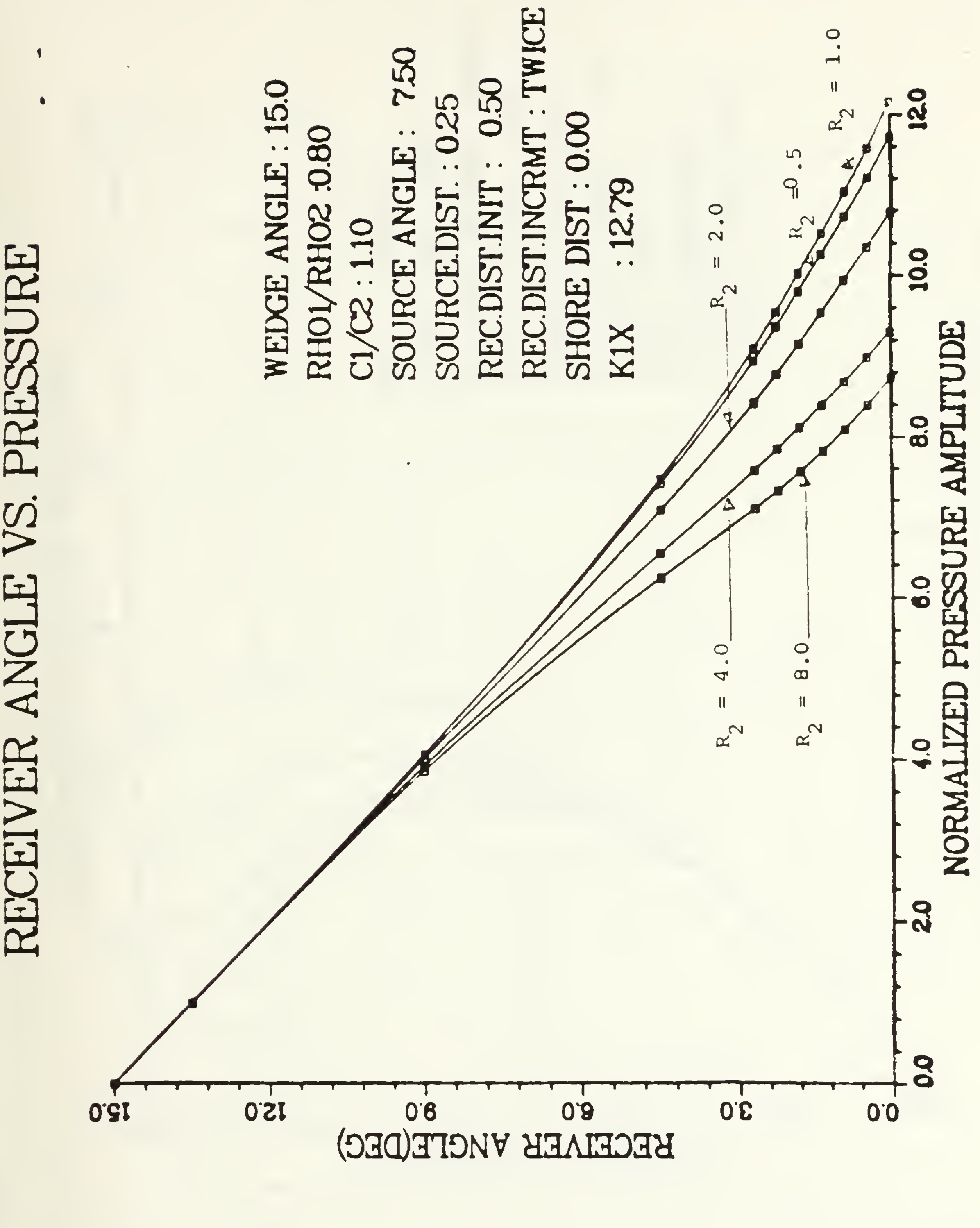

Figure 3.12 Graphs of receiver angle δ versus pressure amplitude with R_2 fixed, R_1 varied

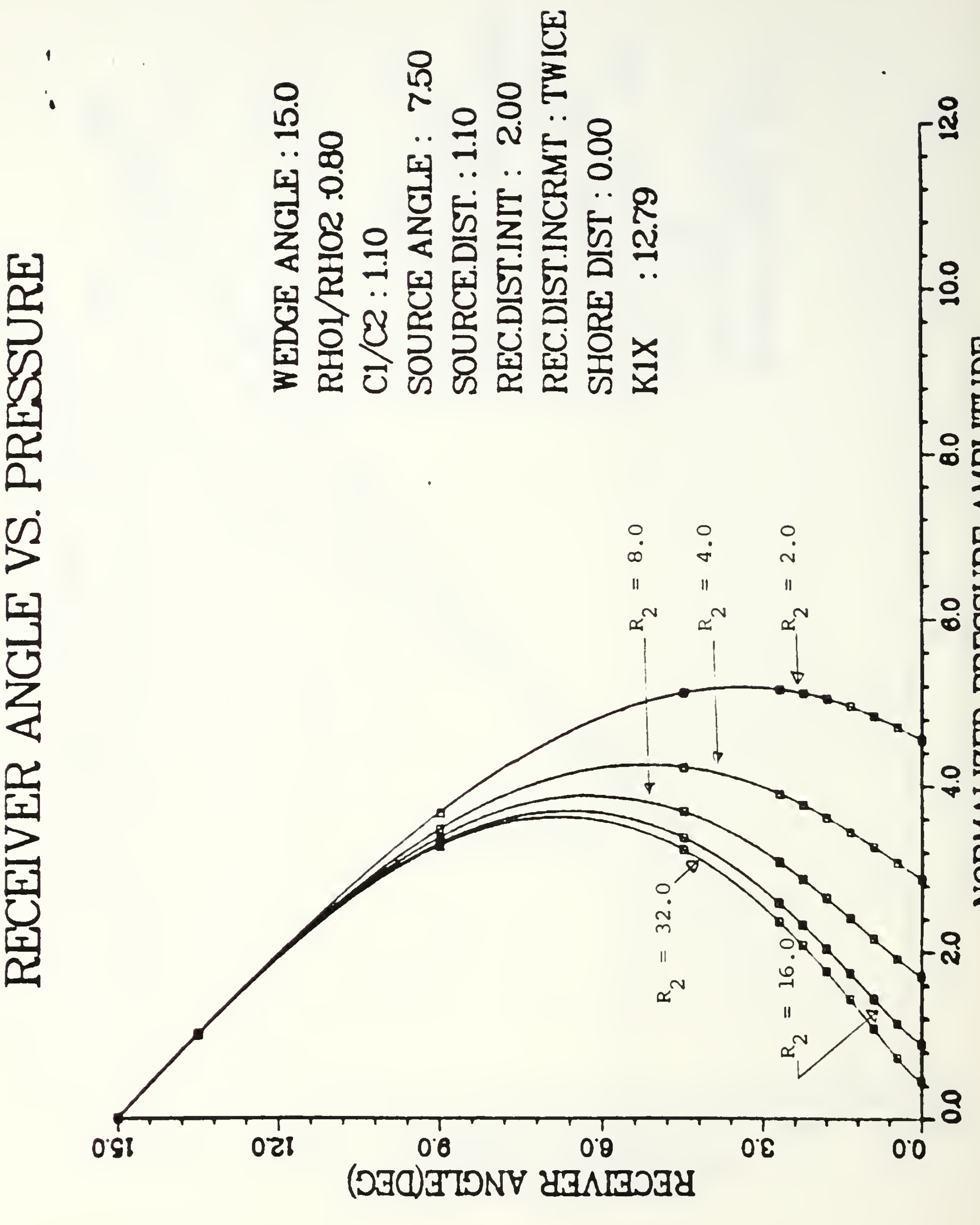

Figure 3.13 Graphs of receiver angle δ versus pressure amplitude with R_2 fixed, R_1 varied

IV. DISCUSSIONS

A. GRAPHICAL OUTPUT

The graphs of normalized pressure amplitude as a function of receiver angle δ were investigated for various source distances R_1 and receiver distances R_2 (Fig. 3.2 to 3.13) while the other parameters are held contstant. For a given wedge angle β and sufficiently small source distance (Fig. 3.8 and 3.12), at all receiver distances, the pressure increases uniformly towards the bottom. For greater source distances, (Fig. 3.9 -3.11) the pressure attains a maximum within the wedge for all receiver distance.

As the receiver distance is increased (Fig. 3.9), a pressure minimum develops between the maximum and the bottom. An important property of the curves of pressure versus receiver angle when there is a maximum and minimum is that, at a specific receiver distance, the pressure above the minimum can be extrapolated to zero pressure on the bottom. (See Fig. 3.10 with R_2 = 32.) This receiver distance is called the "transition point." So far, we do not know the properties of the transition point. We use the transition point for indicating the behavior of the curves when the parameter involved is varied. The transition point appeared twice in some cases, but in the following discussions the first transition point is the only point we will be concerned with. (See Fig. 4.1 for transitions correspond to R_2 = 4.6 and 6.4.)

B. GRAPHS CLASSIFICATION

The development of curves with the source distance (R_1) and the receiver distance (R_2) as variables was observed. As R_1 or R_2 are varied the curve changes from a linear curve to a curve with an observable minimum (Fig. 3.9, R_2 = 5.0) and finally to a curve without a minimum (Fig. 3.9, R_2 = 9.0). Three different types of curves resulted from the series of two-dimensional plotting. They are described below:

1. Type 1 Curves

Type 1 curves (Fig. 4.2) are those where the sound pressure is equal to zero at the surface and maximum at the bottom and is almost linearly dependent on depth. These curves are most pronounced when the source distance is much smaller than the characteristic distance. The closer the source is to the characteristic distance, the more nonlinear the curves (Figs. 3.3 and 3.4).

2. Type 2 Curves

Type 2 curves (Fig. 4.3) are those where the sound pressure is zero at the surface, maximum somewhere between the surface and the bottom with no minimum. These types of curves are generated when the source is placed at a point much greater than the characteristic distance. Type 2

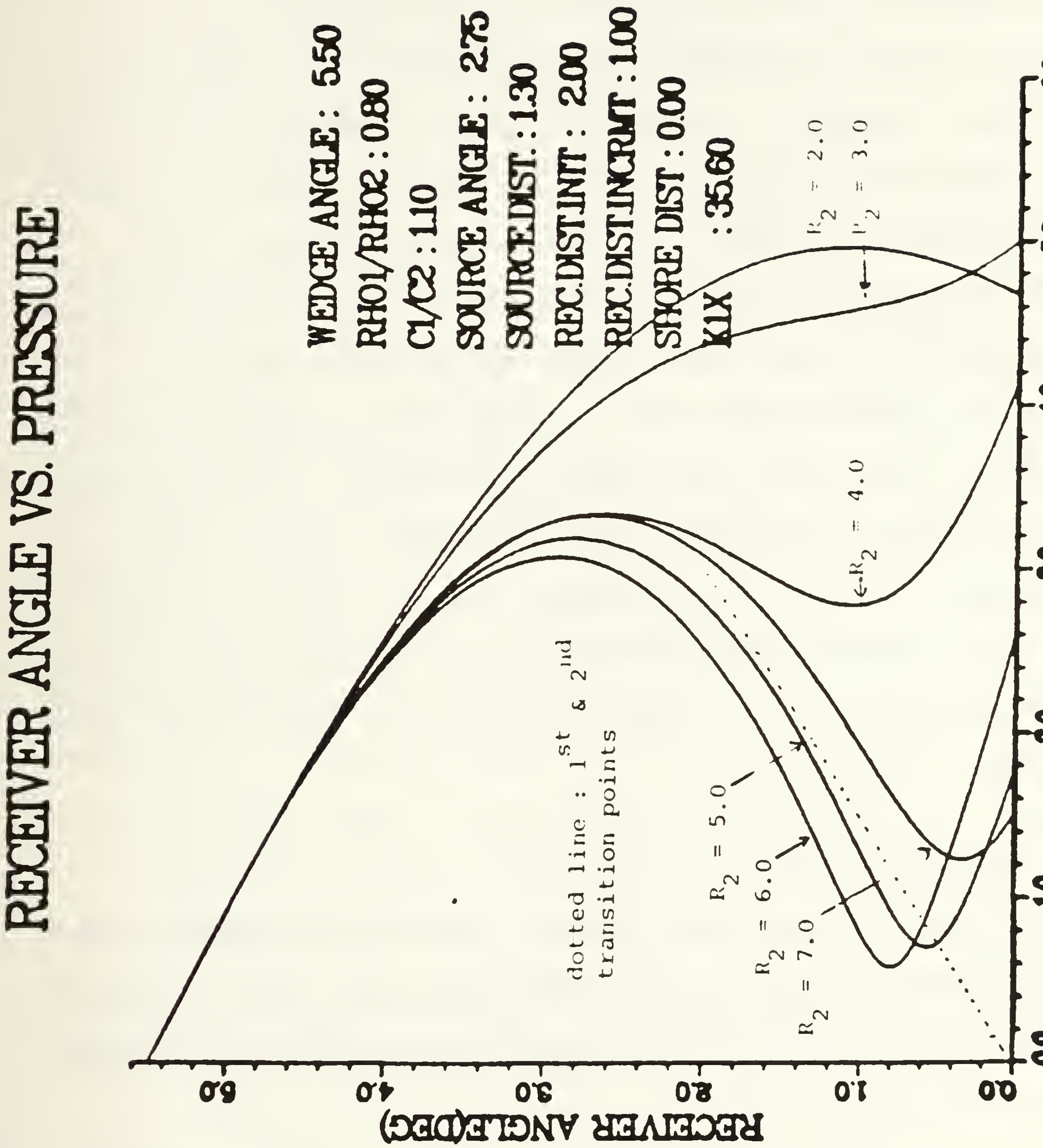

Figure 4.1 The plots where there are two transition points, $R_2=4.6$ is the first and $R_2=6.4$ is the second

curves indicate that the sound energy in the wedge is well collimated and that reflection is negligable.

3. Type 3 Curves

Type 3 curves (Fig. 4.4) are those that have a minimum pressure. These curves occur when the source is a distance slightly greater than, or less than, the characteristic distance. Tables 1, 2, and 3 of Appendix D show the receiver positions at the first transition points. Three different values of β, two different values of ρ_1/ρ_2, and two different values of c_1/c_2 were used in making these tables. The transition point did not occur when $\beta = 15°$, $\rho_1/\rho_2 = 0.90$, $c_1/c_2 = 1.10$. An explanation can be offered using the fact that for these particular sound-speed and density ratios an angle of intromission exists [Ref. 15]. Since the angle of intromission is the grazing angle at which the sound energy is completely transmitted into the slow bottom, it is plausible that no transition point occurs.

C. TRANSITION POINT

By varying the wedge angle β in small increments $\Delta\beta = 0.5°$ starting with $\beta = 5°$, and ending at $\beta = 7°$, it was found that transition occurs for source distances within the range from 1.0 to 1.5.

For $R_1 < 1.0$, no transition point was observed; the curves are the Type 1. For $1.0 < R_1 < 1.5$, the evolution of curves as the receiver distance varied can be explained as follows: first, the receiver is placed near the source and gradually it is shifted further from the source. The minimum in the pressure decreases reaching the point where the curves extrapolate to zero (the first transition point). Further detailed observations were made on this particular facet by varying the source distance and the receiver distances. The results of these observations are tabulated and graphed in Appendices D and E. When the receiver is moved away from the source, the minimum will reach a minimum pressure then the pressure increases until it reaches the point where the curves again can be extrapolated to zero, this is the second transition point (See Fig. 4.1).

For $R_1 > 1.5$, there will be no transition point. The curves are the Type 2.

The transition point as a function of source angle can be observed using the tables in Appendix D. In most cases the greater the source angle γ, the closer the transition point is to the apex. Graphs of transition point as a function of R_1 (Appendix E) indicate that the smaller β the more regular the curves. This is easy to understand because the smaller β, the more accurate the observation of transition point; the greater β the less accurate the data.

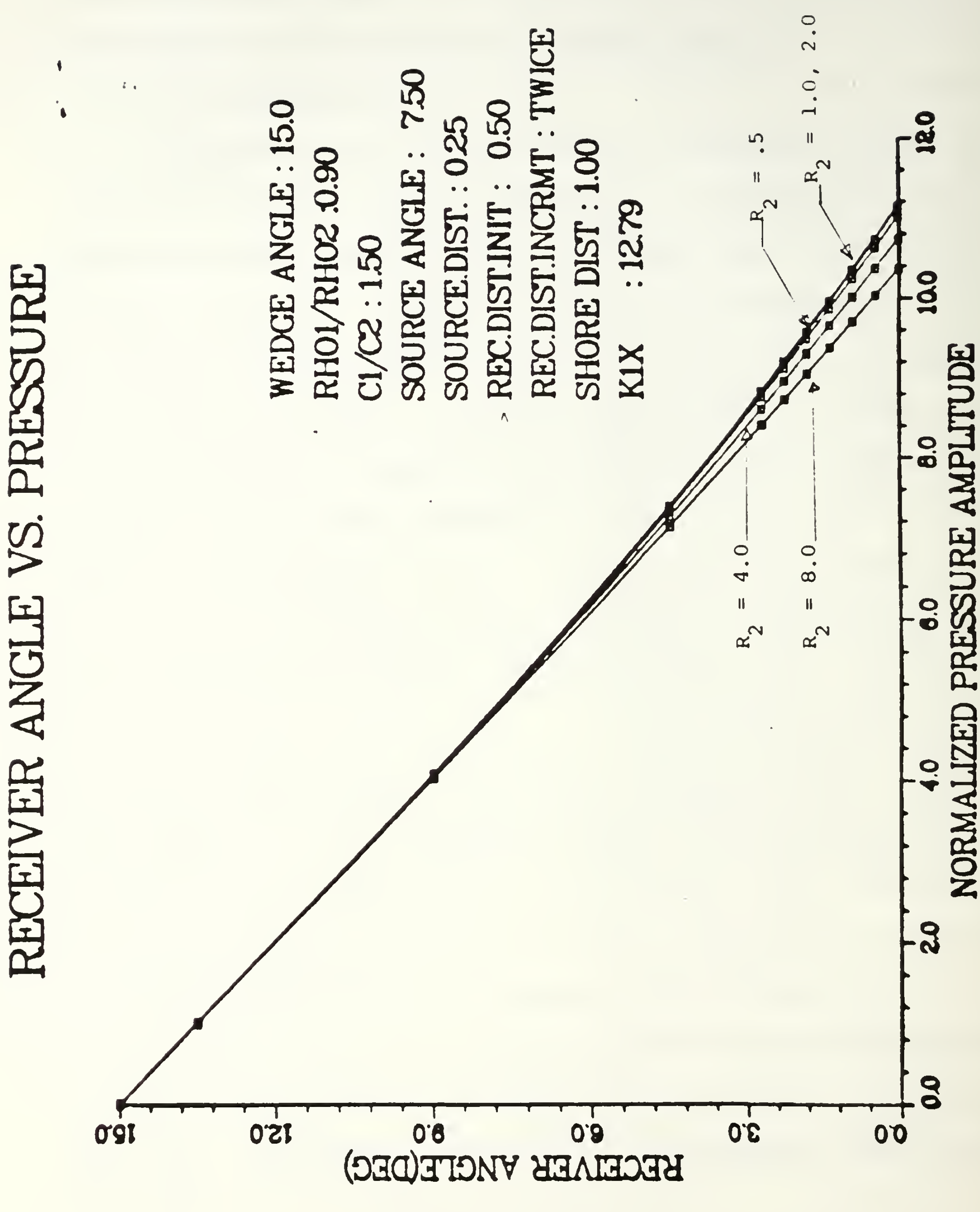

Figure 4.2 Type 2 curves, indicating a pressure amplitude nearly linear with depth

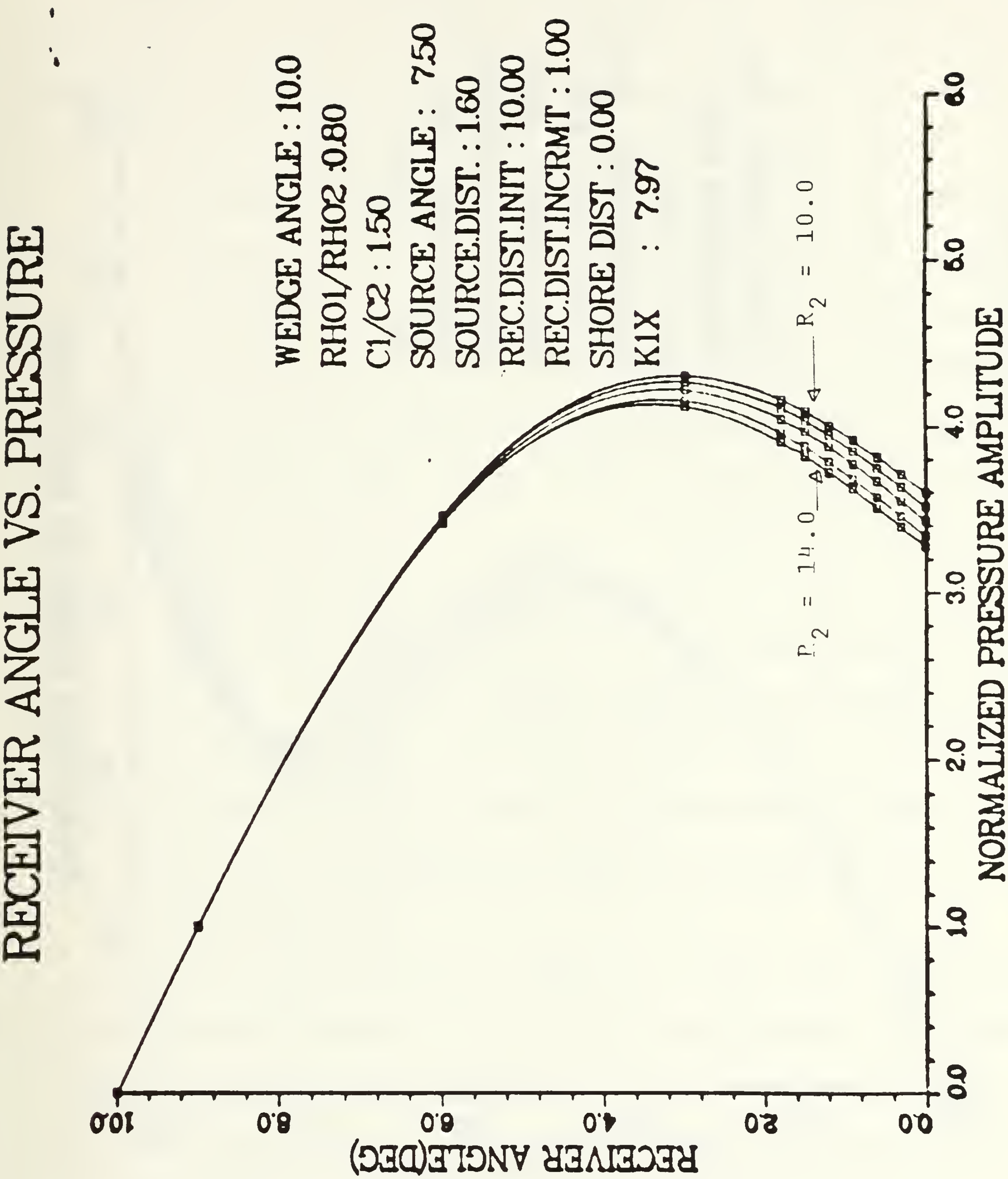

Figure 4.3 Type 2 curves, indicating a well-collimated sound field as the source away from the apex

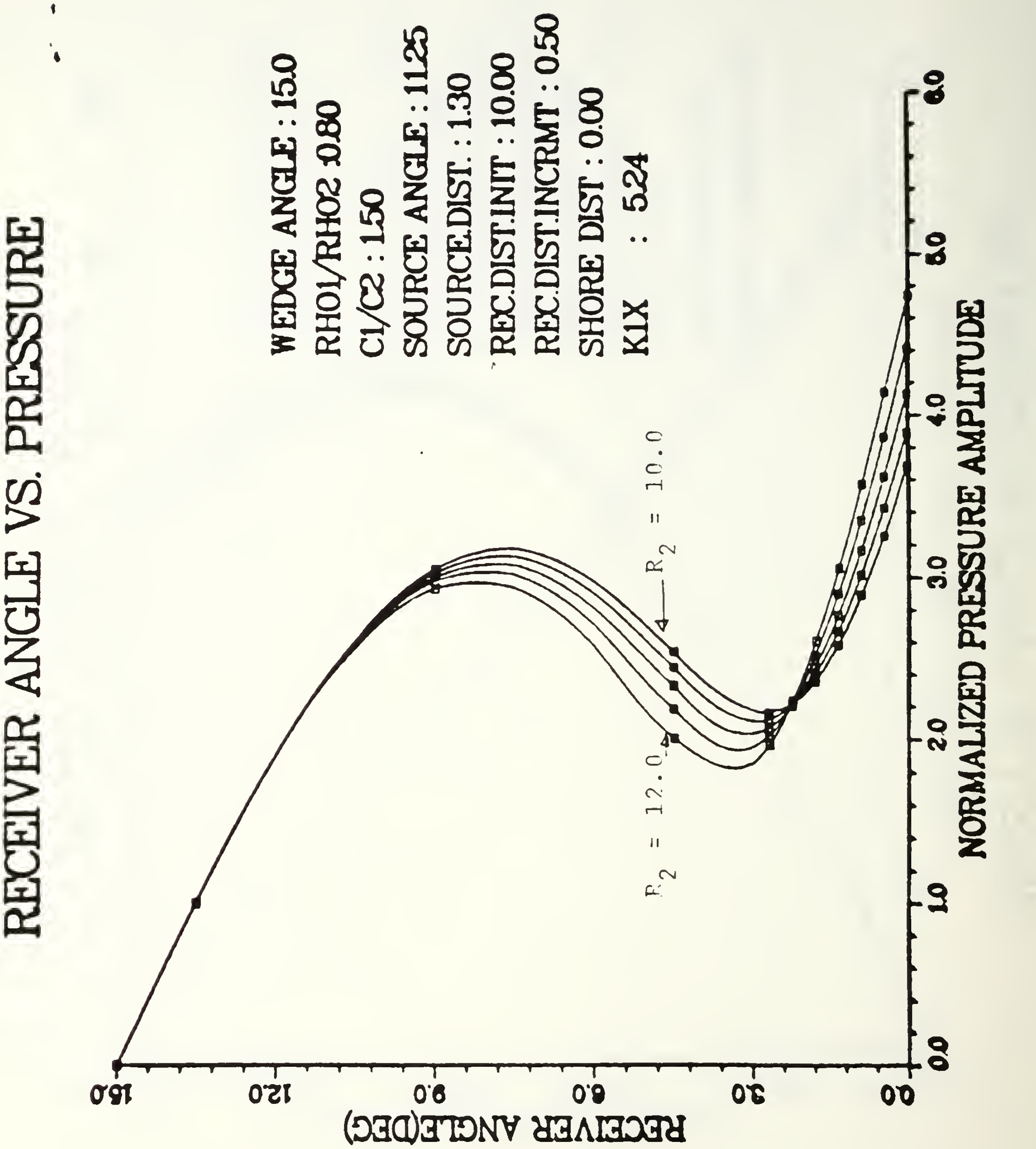

Figure 4.4 Type 3 curves, indicates the presence of reflection and refraction near the bottom

D. PARAMETER VARIATIONS

Variation of parameters was done by changing one parameter of interest while all others were held constant, for fixed source and receiver distances, and plotting the receiver angle versus normalized pressure amplitude.

The parameters β, ρ_1/ρ_2, and c_1/c_2, were held constant and the pressure amplitude was plotted for various δ, R_1, and R_2. The γ's are set at $\beta/4$, $\beta/2$, and $3\beta/4$. Variations in the shore distance (Y_o) can be made because the program is available, but to simplify the investigation, Y_o was set equal to zero for all plots (Fig 4.2 is included as an example for $Y_o \neq 0$).

1. Variations of β

Initially, the values of β investigated were: 6°, 10°, and 15°. The major effect created by altering the value of β is that, for the same values of R_1, ρ_1/ρ_2, and c_1/c_2, the smaller β, the shorter the transition point (see Figs. 3.9 and 3.10, Tables 1, 2, and 3 of Appendix D).

2. Variations of γ

The variations of γ from $\gamma = \beta/4$ (the source is placed near the bottom) to $\gamma = 3\beta/4$ (the source is placed near the surface) are presented in Tables 1, 2, and 3 indicated that the greater γ the shorter the transition point. It is not always true, for instance in Table 1 at $\beta = 6°$, $R_1 = 1.50$, the greater γ the longer transition point, for the rises. (See Appendix D.)

3. Variations of c_1/c_2 and ρ_1/ρ_2

Variations of the acoustical parameters c_1/c_2 and ρ_1/ρ_2 were done, but did not give a significant variation of the sound pressure profile.

V. CONCLUSIONS AND RECOMMENDATIONS

A. CONCLUSIONS

The program DSLOW gives good plots representative of the sound energy distribution within the wedge. The sound energy can be well collimated by the wedge. This phenomenon is strongly affected by the source position. At a source position close enough to the apex, sound energy is distributed linearly with respect to the depth. As the source moved away from the apex, the distribution of sound energy becomes more complex. Sometimes a minimum is found; this minimum may be caused by the presence of sound energy reflected by the bottom.

The source position plays a major role in forming the pressure distribution profile. The pressure distribution is also very sensitive to the parameter variation at small source distances, but it becomes insensitive at large source distance. The characteristic distance must have physical meanings rather than just an arbitrary number, because when the source distance in proximity to the characteristic distance, the model is most sensitive.

The model is restricted when the single precision mode generates round-off error and rough curves which do not allow for accurate analysis.

B. RECOMMENDATIONS

1. Single precision produces good results, but failed in some cases. Double precision would improve the program, but increase the execution time. This must be done by running the program in double precision, and accumulating the result in single precision before plotting the data by DISSPLA.
2. It is suggested that the program be run using more realistic parameters and observing the effects on the characteristic distance and transition point.
3. Further study validating DSLOW in comparison with experimental results is suggested.

APPENDIX A
DSLOW ALGORITHM

The pressure amplitude calculation

$$N_1 = \mathrm{INT}[180/\beta] \qquad \text{(eqn A.1)}$$

$$K_1X = \frac{\pi}{2\tan\beta\ \tan[\arccos(c_2/c_1)]} \qquad \text{(eqn A.2)}$$

$$AL = \alpha/K_2 = 0.0001 \quad \text{(constant)} \qquad \text{(eqn A.3)}$$

$$D_2 = Y_o{}^2 + R_1{}^2 + R_2{}^2 \qquad \text{(eqn A.4)}$$

$$R_3 = 2R_1R_2 \qquad \text{(eqn A.5)}$$

$$R_8 = \sqrt{D_2 - R_3 \cos[(N-1)\beta + \gamma - \delta]} \qquad \text{(eqn A.6)}$$

$$R_9 = \sqrt{D_2 - R_3 \cos[(N-1)\beta + \gamma + \delta]} \qquad \text{(eqn A.7)}$$

$$S_2 = (-1)^{\mathrm{INT}(N_1/2)} \qquad \text{(eqn A.8)}$$

$$W_1 = 2AL(c_1/c_2)^2 \qquad \text{(eqn A.9)}$$

$$SI = |\{R_1 \sin[(N-1)\beta + \gamma] - 2[\mathrm{INT}((N-1)/2)\beta \qquad \text{(eqn A.10)}$$

$$+ R_2 \sin[2\mathrm{INT}((N-1)/2)\beta - \delta]\}|/R_8$$

$$CI = \sqrt{(1-SI^2)} \qquad \text{(eqn A.11)}$$

$$T = SI/D_1 \qquad \text{(eqn A.12)}$$

$$W_o = (-c_2 + c_1/c_2) \qquad \text{(eqn A.13)}$$

$$Y = \sqrt{W_o^2 + W_1^2} \qquad \text{(eqn A.14)}$$

$$Z = |W_o| \qquad \text{(eqn A.15)}$$

$$Y_1 = \sqrt{(Y + W_o)/2} \qquad \text{(eqn A.16)}$$

$$Y_2 = \sqrt{(Y - W_o)/2} \qquad \text{(eqn A.17)}$$

$$Z_1 = \frac{T_1 - Y_2}{(T - Y_2)^2 + Y_1^2} \qquad \text{(eqn A.18)}$$

$$Z_2 = \frac{Y_1}{(T - Y_2)^2 + Y_1^2} \qquad \text{(eqn A.19)}$$

$$Z_5 = \frac{(T^2 - Y_2)^2 - Y_1^2}{(T^2 - Y_2)^2 + Y_1^2} \qquad \text{(eqn A.20)}$$

$$Z_6 = \frac{2Y_1T}{(T^2 - Y_2)^2 + Y_1^2} \qquad \text{(eqn A.21)}$$

$$P_1 = \sum_{n=1}^{N_1} (-1)^{INT(N/2)}\{Z_5 \cos(R_{8n}K_1X) + Z_6 \sin(R_{8n}K_1X\}/R_{8n} \qquad \text{(eqn A.22)}$$

$$P_2 = \sum_{n=1}^{N_1} (-1)^{INT(N/2)}\{-Z_5 \sin(R_{8n}K_1X) + Z_6 \cos(R_{8n}K_1X\}/R_{8n} \qquad \text{(eqn A.23)}$$

$$P_3 = \sum_{n=1}^{N_1} (-1)^{INT(N/2)}\{Z_5 \cos(R_{9n}K_1X) + Z_6 \sin(R_{9n}K_1X\}/R_{9n} \qquad \text{(eqn A.24)}$$

$$P_4 = \sum_{n=1}^{N_1} (-1)^{INT(N/2)} \{-Z_5 \sin(R_{9n} K_1 X) + Z_6 \cos(R_{9n} K_1 X\} / R_{9n} \qquad \text{(eqn A.25)}$$

$$P_5 = P_1 + P_2 \qquad \text{(eqn A.26)}$$

$$P_6 = P_3 + P_4 \qquad \text{(eqn A.27)}$$

$$P_{tot} = R_1 \sqrt{P_5^2 + P_6^2} \qquad \text{(eqn A.28)}$$

APPENDIX B

DSLOW PROGRAM

```
************************************************************************
**     THIS PROGRAM CALLED DSLOW IS CALCULATING THE SOUND PRESSURE     **
**     WITHIN THE WEDGE OVERLYING SLOW BOTTOM FLUID AND DOWN-SLOPE     **
**                           DIRECTION                                 **
************************************************************************
-
-      INTEGER    A,I,I1,M,N,S1,S2,N1,J,K,P
-      REAL*4               B,CC,C2,D,D1,D2,G,PI,P1,P2,Q1,R1,R2,T,
-     *                     T4,T6,W0,W1,Y0,Y1,Y2,Z1,Z2,Z3,Z4,Z5,Z6,
-     *                     T1(80),R8(80),R9(80),S(30),C(30),E(30),AT(30),
-     *                     F(30),Y,Z,R3,AL,PZ(30),DZ(30),V,DX,XP,DD,PN(30)
-      REAL*4 TQQ,TQQ1,TQQ2,TQQ3
-      PI =ACOS(-1.0D00)
************************************************************************
**     INPUT PARAMETERS                                                 **
************************************************************************
C      B = WEDGE ANGLE (DEG)
C      G = SOURCE ANGLE (DEG)
C      D = RECEIVER ANGLE (DEG)
C      N1= # OF IMAGE POINTS
C      R1 = SOURCE DISTANCE (IN CHARACTERISTIC DISTANCES)
C      R2 = RECEIVER DISTANCE (IN CHARACTERISTIC DISTANCES)
C      Y0 = APEX DISTANCE (IN CHARACTERISTIC DISTANCES)
C      D1 = RHO 1/RHO 2
C      CC = C-1/C-2
C      AL = ALPHA/K2
C      A  = # OF RECEIVER POSITIONS
************************************************************************
**     INITIAL INPUT & RELATIONS                                       **
************************************************************************
C      Y0 = 0.00
-      R2 = 9.00
-      DO 111 P=1,6
C      B = 10.0
-      B = 10.0
C      G = 3*B/4
C      G = 2*B/4
-      G = 1*B/4
-      D = 0.0
C      R1 = 0.95
-      R1 = 1.10
C      R1 = 1.00
-      R1 = 0.75
C      R2 = 1.01
C      R2 = 1.20
C      R2 = 1.50
C      R2 = 2.00
C      R2 = 5.00
-      Y0 = 0.00
-      D1 = 0.80
-      CC = 1.10
-      AL = 0.0001
-      A = 10
************************************************************************
**     THE MAIN PROGRAM CALCULATES UPPER AND LOWER PATH OF RAYS        **
************************************************************************
-      K  = 0
-      N1 = INT(180./B)
-      T6 = 180./PI
-      B = B/T6
-      G = G/T6
-      C2 = CC**2
-      D2 = (Y0*Y0)+(R1*R1)+(R2*R2)
-      R3 = 2.*R1*R2
C      T4 = PI/(2*TAN(ACOS(1/CC))*TAN(B))
-      TQQ = TAN(B)
-      TQQ1 = ACOS(1/CC)
-      TQQ2 = TAN(TQQ1)
-      TQQ3 = 2.*TQQ2*TQQ
-      T4 = PI/TQQ3
```

```
C     K1X= PI/(2*TOO*TOO2)
-     D2 = Y0*Y0+R1*R1+R2*R2
-     Q1 = 1/DSQRT(2.0D00)
C240  FORMAT(' NOP    ',7X,'THETA(N) ',7X,'IMGE SR R8  ',7X,
C    *    'IMGE SR R9 ')
C     WRITE (6,240)
-241  FORMAT('   ')
-     WRITE (6,241)
-250  FORMAT(' WEDGE ANGLE =    ',F5.2,1X,' SOURCE ANGLE =  ',F5.2)
-     WRITE (6,250) B*T6,G*T6
-251  FORMAT(' SOURCE DISTANCE=',F4.2,1X,'RECEIVER DISTANCE= ',F6.2,1X,
-    *    ' SHORE DISTANCE= ',F4.2)
-     WRITE (6,251) R1,R2,Y0
-270  FORMAT(' RHO1/RHO2=',F5.2,5X,' C1/C2=',F5.2,5X,' ALPHA/K2=',F8.4)
-     WRITE (6,270) D1,CC,AL
-271  FORMAT(' K1X   =  ',F5.2)
-     WRITE (6,271) T4
-272  FORMAT('  ')
-     WRITE (6,272)
-800  FORMAT(1X,'REC.POS',2X,' REC.ANGLE ',2X,'PRES.AMPLITUDE ',3X,
-    *    'PHASE ANGLE ',4X,'NORM.PRESS')
-     WRITE (6,800)
-801  FORMAT('   ')
-     WRITE (6,801)
-     DO 10  M = 0,A
-        D = M*B/A
-        DD=B/A
-        V =2*B/10
-        IF(D.LT.V) GOTO 110
-        IF(D.GE.V) GOTO 120
-110     DX = D
-      DO 15  J = 1,10
-        D  = DX+(J-1)*B/(10*A)
-        DD = B/(10*A)
-120     S1 = 1.0
-        DO 20  N = 1,N1
-           IF(S1.GT.0) T1(N)=(N-1)*B+G
-           IF(S1.LT.0) T1(N)=N*B-G
-           S1 = - S1
-           R8(N) = SQRT(D2-R3*COS(T1(N)-D))
-           R9(N) = SQRT(D2-R3*COS(T1(N)+D))
C310  FORMAT(3X,I2  ,5X,F5.2,4X,F6.4,6X,F6.4)
C     WRITE (6,310) N,T1(N),R8(N),R9(N)
-20   CONTINUE
-        P1 = 0.0
-        P2 = 0.0
-        DO 30  N = 1,N1
-           S2 = (-1)**(INT(N/2))
-           W1 = 2*C2*AL
-           I1 = INT((N-1)/2)
-           DO 40  I = 1,I1
-              S(I) = ABS(R1*SIN(T1(N)-2*I*B)
-    *                +R2*SIN(2*I*B-D))/R8(N)
-              C(I) = SQRT(1-(S(I)*S(I)))
-              T = S(I)/D1
-              W0 = (-C2+(C(I)*C(I)))
-              Y = SQRT((W0*W0)+(W1*W1))
-              Z =ABS(W0)
-              IF(Y.LE.Z) Y = Z
-              Y1 = Q1*SQRT(Y+W0)
-              Y2 = -Q1*SQRT(Y-W0)
-              Z1 = T-Y2
-              Z2 = -Y1
C             Z12= CMPLX(Z1R,Z2I)
-              Z3 = Z1/(Z1*Z1+Z2*Z2)
-              Z4 =-Z2/(Z1*Z1+Z2*Z2)
-              Z1 = T+Y2
-              Z2 = Y1
C             Z13= CMPLX(Z3R,Z4I)
-              Z5 = Z1*Z3-Z2*Z4
-              Z6 = Z1*Z4+Z2*Z3
C             Z14= CMPLX(Z5R,Z6I)
-              E(I) = Z5
-              F(I) = Z6
C400  FORMAT(' NOP  ',5X,'I ',5X,'ARSIN(S(I)*T6)',5X,'E(I)',
C    *     5X,'F(I)',5X,
C    *     ' DSQRT(E(I)*E(I)+F(I)*F(I))',5X,'T6*ATAN(F(I)/E(I))')
C     WRITE (6,400)
```

```
C420   FORMAT(3X,I2,6X,I2,5X,F6.4,10X,F6.4,3X,F6.4,3X,F6.4,10X,F7.4)
C      WRITE (6,420) N,I, ASIN(S(I))*T6,E(I),F(I)
C    *              SQRT(E(I)*E(I)+F(I)*F(I)),ATAN(F(I)/E(I))
-   40 CONTINUE
-              Z1 = 0
-              Z2 = 0
-              Z3 = 0
-              Z4 = 0
-              Z5 = 1
-              Z6 = 0
-          IF(N.LE.2.00) GOTO 50
-          DO 45  I = 1, I1
-              Z1 = E(I)
-              Z2 = F(I)
-              Z3 = Z5
-              Z4 = Z6
-              Z5 = Z1*Z3-Z2*Z4
-              Z6 = Z1*Z4+Z2*Z3
-   45  CONTINUE
-   50         Z1 = Z5
-              Z2 = Z6
-              T  = T4*R8(N)
-              Z3 = COS(T)
-              Z4 = -SIN(T)
-              Z5 = Z1*Z3-Z2*Z4
-              Z6 = Z1*Z4+Z2*Z3
-              P1 = P1+S2*Z5/R8(N)
-              P2 = P2+S2*Z6/R8(N)
C500   FORMAT(' NO.OF I.P ',3X,'RE(REFL)= ',3X,'IM(REFL)= ')
C      WRITE (6,500)
C510   FORMAT(3X,I2,6X,F6.4,6X,F6.4)
C      WRITE (6,510) N,S2*Z1,S2*Z2
C600   FORMAT(' I',5X,'ARCSIN(S(I))*T6=',3X,'E(I)',5X,'F(I)',5X,'EF',
C    *        5X,' AN2 ')
C      WRITE (6,600)
-              I1=I1+1
-      DO 60 I = 1, I1
-              S(I) = ABS(R1*SIN(T1(N)-2*(I-1)*B)
-    *                  + R2*SIN(2*(I-1)*B+D))/R9(N)
-              C(I) = SQRT(1-S(I)*S(I))
-              T = S(I)/D1
-              W0 = -C2+C(I)*C(I)
-              Y = SQRT((W0*W0)+(W1*W1))
-              Z = ABS(W0)
-              IF(Y.LE.Z) Y = Z
-              Y1 = Q1*SQRT(Y+W0)
-              Y2 = -Q1*SQRT(Y-W0)
-              Z1 = T-Y2
-              Z2 = -Y1
-              Z3 = Z1/(Z1*Z1+Z2*Z2)
-              Z4 = - Z2/(Z1*Z1+Z2*Z2)
-              Z1 = T+Y2
-              Z2 = Y1
-              Z5 = Z1*Z3-Z2*Z4
-              Z6 = Z1*Z4+Z2*Z3
-              E(I) = Z5
-              F(I) = Z6
-              AN1= ASIN(S(I))*T6
-              EF = SQRT(E(I)*E(I)+F(I)*F(I))
-              AN2= ATAN(F(I)/E(I))*T6
C610   FORMAT(2X,I2,5X,F6.4,5X,F6.4,5X,F6.4,5X,F6.4,5X,F7.4)
C      WRITE (6,610) I,AN1,E(I),F(I),EF,AN2
-   60 CONTINUE
-              Z1 = 0
-              Z2 = 0
-              Z3 = 0
-              Z4 = 0
-              Z5 = 1
-              Z6 = 0
-      DO 80 I = 1,I1
-              Z1 = E(I)
-              Z2 = F(I)
-              Z3 = Z5
-              Z4 = Z6
-              Z5 = Z1*Z3-Z2*Z4
-              Z6 = Z1*Z4+Z2*Z3
-   80 CONTINUE
-              Z1 = Z5
```

```
-            Z2 = Z6
-            T  = T4*R9(N)
-            Z3 = COS(T)
-            Z4 = -SIN(T)
-            Z5 = Z1*Z3-Z2*Z4
-            Z6 = Z1*Z4+Z2*Z3
-            P1 = P1+S2*Z5/R9(N)
-            P2 = P2+S2*Z6/R9(N)
C700  FORMAT(' LOWER PATH NO=',3X,'RE(REFL)= ',3X,'IM(REFL)= ')
C     WRITE ( 6,700)
C710  FORMAT(6X,I2,12X,F6.4,12X,F6.4)
C     WRITE (6,710) N,S2*Z1,S2*Z2
-  30 CONTINUE
-     K = K+1
-     DZ(K)=D*T6
-     PZ(K)=SQRT(P1*P1+P2*P2)*R1
-     AT(K)=ATAN(P2/P1)
C     WRITE (6,810) K,DZ(K),PZ(K),ATAN(P2/P1),PN(K)
-810  FORMAT(6X,I3,11X,F5.2,12X,F7.4,12X,F7.4,10X,F7.4)
-15   CONTINUE
-10   CONTINUE
-     DO 31 L=1,29
-     XP=PZ(28)
-     PN(L)=PZ(L)/XP
-     WRITE (6,811) L,DZ(L),PZ(L),AT(L),PN(L)
-811  FORMAT(2X,I3,7X,F5.2,8X,F9.6,8X,F9.6,6X,F9.6)
-31   CONTINUE
C     Y0=Y0+0.5
-     R2=R2*0.50
-111  CONTINUE
-     STOP
-     END
*******************************************************************************
**    A SUBPROGRAM FOR PLOTTING BY TEK618OR SHERPA                          **
*******************************************************************************
C     CALL MEDBUF
C     CALL TEK618
C     CALL COMPRS
C     CALL NOBRDR
C     CALL PAGE(15.,12.)
C     CALL AREA2D(11.,9.)
C     CALL HEIGHT(.2)
C     CALL XNAME('NORMALIZED PRESSURE AMPLITUDE$',29)
C     CALL YNAME('RECEIVER ANGLE(DEG)$',19)
C     CALL YTICKS(5)
C     CALL XTICKS(5)
C     CALL GRAF(0.,0.10,0.50,0.,5.0,15.0)
C     CALL GRAF(0.,10.,50.0,0.,5.0,10.0)
C     CALL GRAF(0.,3.0,15.0,0.,3.0,15.0)
C     CALL DOT
C     CALL GRID(2,2)
C     CALL HEADIN('REC.ANGLE VS. PRESSURES',-100,1.8,1)
C     CALL MESSAG('WEDGE ANGLE: $',100,8.,7.)
C     CALL MESSAG('15.0$',100,'ABUT','ABUT')
C     CALL MESSAG('RHO1/RHO2: $',100,8.,6.5)
C     CALL MESSAG('0.80 $',100,'ABUT','ABUT')
C     CALL MESSAG('C1/C2: $',100,8.,6.0)
C     CALL MESSAG('1.50$',100,'ABUT','ABUT')
C     CALL MESSAG('SOURCE ANGLE: $',100,8.,5.5)
C     CALL MESSAG('11.25$',100,'ABUT','ABUT')
C     CALL MESSAG(' 7.50$',100,'ABUT','ABUT')
C     CALL MESSAG(' 3.75$',100,'ABUT','ABUT')
C     CALL MESSAG(' 7.50$',100,'ABUT','ABUT')
C     CALL MESSAG('SOURCE DIST.: $',100,8.,5.)
C     CALL MESSAG('0.25 $',100,'ABUT','ABUT')
C     CALL MESSAG('1.10 $',100,'ABUT','ABUT')
C     CALL MESSAG('1.60$',100,'ABUT','ABUT')
C     CALL MESSAG('0.95 $',100,'ABUT','ABUT')
C     CALL MESSAG('REC.DIST.INIT: $',100,8.,4.5)
C     CALL MESSAG('0.50 $',100,'ABUT','ABUT')
C     CALL MESSAG('1.00 $',100,'ABUT','ABUT')
C     CALL MESSAG('3.00 $',100,'ABUT','ABUT')
C     CALL MESSAG('3.00 $',100,'ABUT','ABUT')
C     CALL MESSAG('REC.DIST.INCRMT : $',100,8.,4.0)
C     CALL MESSAG('TWICE$',100,'ABUT','ABUT')
C     CALL MESSAG('2.00$',100,'ABUT','ABUT')
C     CALL MESSAG('SHO.DIST.INIT: $',100,8.,3.5)
C     CALL MESSAG('1.00 $',100,'ABUT','ABUT')
```

```
C      CALL MESSAG('SHO.DIST: $',100,8.,3.5)
C      CALL MESSAG('0.00 $',100,'ABUT','ABUT')
C      CALL RESET('ALL')
C      CALL PARA3
C      CALL POLY3
C      CALL NOCHEK
C      CALL CURVE(PN,DZ,29,0)
C111   CONTINUE
C      CALL ENDPL(0)
C      CALL DONEPL
C      STOP
C      END

**************************************************************************
** For plotting the calculations result on TEK618 or Sherpa, erase     **
** the proper C's in DISSPLA subprogram above. Put C's in front of     **
** 111 CONTINUE, STOP and END in Main Program.                         **
**************************************************************************
```

APPENDIX C
NUMERICAL RESULTS OF DSLOW

WEDGE ANGLE = 10.00 SOURCE ANGLE = 2.50
SOURCE DISTANCE=0.75 RECEIVER DISTANCE= 9.00 SHORE DISTANCE= 0.00
RHO1/RHO2= 0.80 C1/C2= 1.10 ALPHA/K2= 0.0001
K1X = 19.44

REC.POS	REC.ANGLE	PRES.AMPLITUDE	PHASE ANGLE	NORM.PRESS
1	0.00	0.007611	-1.129606	6.792701
2	0.10	0.007390	-1.108071	6.595129
3	0.20	0.007175	-1.085083	6.403362
4	0.30	0.006965	-1.061422	6.215911
5	0.40	0.006763	-1.037255	6.035660
6	0.50	0.006563	-1.011464	5.857465
7	0.60	0.006374	-0.984591	5.688235
8	0.70	0.006191	-0.957120	5.524890
9	0.80	0.006014	-0.928227	5.367038
10	0.90	0.005844	-0.898359	5.215738
11	1.00	0.005681	-0.867409	5.070300
12	1.10	0.005526	-0.835250	4.931440
13	1.20	0.005379	-0.802517	4.800441
14	1.30	0.005239	-0.768184	4.675240
15	1.40	0.005107	-0.732669	4.557538
16	1.50	0.004983	-0.696848	4.446829
17	1.60	0.004866	-0.659586	4.342858
18	1.70	0.004759	-0.622856	4.247226
19	1.80	0.004658	-0.583461	4.156956
20	1.90	0.004566	-0.545011	4.074470
21	2.00	0.004482	-0.505302	3.999775
22	3.00	0.004003	-0.113330	3.572277
23	4.00	0.003919	0.201979	3.497443
24	5.00	0.003841	0.413213	3.427758
25	6.00	0.003550	0.547851	3.168519
26	7.00	0.002981	0.632015	2.660608
27	8.00	0.002149	0.680885	1.917873
28	9.00	0.001121	0.697709	1.000000
29	10.00	0.000000	-0.048596	0.000029

WEDGE ANGLE = 10.00 SOURCE ANGLE = 2.50
SOURCE DISTANCE=0.75 RECEIVER DISTANCE= 4.50 SHORE DISTANCE= 0.00
RHO1/RHO2= 0.80 C1/C2= 1.10 ALPHA/K2= 0.0001
K1X = 19.44

REC.POS	REC.ANGLE	PRES.AMPLITUDE	PHASE ANGLE	NORM.PRESS
1	0.00	0.037832	1.537560	7.554441
2	0.10	0.037361	1.553782	7.460239
3	0.20	0.036906	1.569994	7.369551
4	0.30	0.036460	-1.555159	7.280349
5	0.40	0.036019	-1.538568	7.192361
6	0.50	0.035594	-1.521979	7.107576
7	0.60	0.035178	-1.505386	7.024406
8	0.70	0.034766	-1.488472	6.942234
9	0.80	0.034371	-1.471694	6.863304
10	0.90	0.033981	-1.454889	6.785389
11	1.00	0.033602	-1.437988	6.709667
12	1.10	0.033229	-1.420986	6.635274
13	1.20	0.032867	-1.404230	6.562953
14	1.30	0.032511	-1.387417	6.491957
15	1.40	0.032163	-1.370529	6.422443
16	1.50	0.031823	-1.353691	6.354450
17	1.60	0.031492	-1.336905	6.288318
18	1.70	0.031166	-1.320334	6.223366
19	1.80	0.030846	-1.303701	6.159449
20	1.90	0.030532	-1.287225	6.096689
21	2.00	0.030226	-1.270993	6.035670
22	3.00	0.027368	-1.116021	5.464833
23	4.00	0.024629	-0.981865	4.917889
24	5.00	0.021663	-0.872103	4.325723
25	6.00	0.018253	-0.786891	3.644764
26	7.00	0.014269	-0.724721	2.849282
27	8.00	0.009828	-0.682756	1.962534
28	9.00	0.005008	-0.660769	1.000000
29	10.00	0.000000	0.273944	0.000001

WEDGE ANGLE = 10.00 SOURCE ANGLE = 2.50
SOURCE DISTANCE=0.75 RECEIVER DISTANCE= 2.25 SHORE DISTANCE= 0.00
RHO1/RHO2= 0.80 C1/C2= 1.10 ALPHA/K2= 0.0001
K1X = 19.44

REC.POS	REC.ANGLE	PRES.AMPLITUDE	PHASE ANGLE	NORM.PRESS
1	0.00	0.224816	1.084841	6.519929
2	0.10	0.224336	1.092171	6.505989
3	0.20	0.223838	1.099430	6.491551
4	0.30	0.223305	1.106651	6.476104
5	0.40	0.222733	1.113891	6.459502
6	0.50	0.222113	1.121132	6.441518
7	0.60	0.221472	1.128275	6.422938
8	0.70	0.220805	1.135338	6.403585
9	0.80	0.220096	1.142416	6.383023
10	0.90	0.219349	1.149437	6.361359
11	1.00	0.218573	1.156374	6.338860
12	1.10	0.217751	1.163238	6.315019
13	1.20	0.216893	1.170144	6.290153
14	1.30	0.216000	1.176949	6.264237
15	1.40	0.215070	1.183646	6.237287
16	1.50	0.214095	1.190398	6.209000
17	1.60	0.213090	1.197003	6.179859
18	1.70	0.212046	1.203545	6.149565
19	1.80	0.210963	1.210009	6.118167
20	1.90	0.209839	1.216443	6.085560
21	2.00	0.208671	1.222806	6.051688
22	3.00	0.194767	1.281938	5.648450
23	4.00	0.176765	1.333861	5.126376
24	5.00	0.154712	1.377699	4.486838
25	6.00	0.128893	1.413359	3.738033
26	7.00	0.099744	1.441621	2.892702
27	8.00	0.068024	1.461364	1.972762
28	9.00	0.034481	1.473173	1.000000
29	10.00	0.000000	-1.243458	0.000001

WEDGE ANGLE = 10.00 SOURCE ANGLE = 2.50
SOURCE DISTANCE=0.75 RECEIVER DISTANCE= 1.13 SHORE DISTANCE= 0.00
RHO1/RHO2= 0.80 C1/C2= 1.10 ALPHA/K2= 0.0001
K1X = 19.44

REC.POS	REC.ANGLE	PRES.AMPLITUDE	PHASE ANGLE	NORM.PRESS
1	0.00	1.900229	-0.125102	4.791066
2	0.10	1.923264	-0.119954	4.849142
3	0.20	1.944952	-0.114742	4.903825
4	0.30	1.965253	-0.109495	4.955010
5	0.40	1.984233	-0.104208	5.002865
6	0.50	2.001945	-0.098897	5.047521
7	0.60	2.018349	-0.093551	5.088881
8	0.70	2.033438	-0.088218	5.126925
9	0.80	2.047371	-0.082850	5.162055
10	0.90	2.060028	-0.077489	5.193968
11	1.00	2.071478	-0.072146	5.222836
12	1.10	2.081736	-0.066788	5.248699
13	1.20	2.090869	-0.061446	5.271727
14	1.30	2.098818	-0.056122	5.291768
15	1.40	2.105642	-0.050809	5.308975
16	1.50	2.111385	-0.045508	5.323455
17	1.60	2.115994	-0.040234	5.335076
18	1.70	2.119550	-0.034997	5.344040
19	1.80	2.122012	-0.029773	5.350248
20	1.90	2.123518	-0.024576	5.354045
21	2.00	2.123900	-0.019431	5.355009
22	3.00	2.074631	0.029804	5.230785
23	4.00	1.939167	0.074109	4.889239
24	5.00	1.730041	0.112477	4.361967
25	6.00	1.459312	0.144356	3.679378
26	7.00	1.138785	0.169405	2.871230
27	8.00	0.780462	0.187392	1.967786
28	9.00	0.396619	0.198255	1.000000
29	10.00	0.000001	-1.531829	0.000002

WEDGE ANGLE = 10.00 SOURCE ANGLE = 2.50 SHORE DISTANCE= 0.00
SOURCE DISTANCE=0.75 RECEIVER DISTANCE= 0.56 ALPHA/K2= 0.0001
RHO1/RHO2= 0.80 C1/C2= 1.10
K1X = 19.44

REC.POS	REC.ANGLE	PRES.AMPLITUDE	PHASE ANGLE	NORM.PRESS
1	0.00	3.992624	0.306449	5.479548
2	0.10	4.016742	0.310540	5.512648
3	0.20	4.038875	0.314667	5.543023
4	0.30	4.059057	0.318822	5.570723
5	0.40	4.077303	0.323001	5.595763
6	0.50	4.093628	0.327198	5.618168
7	0.60	4.107439	0.331284	5.637122
8	0.70	4.120035	0.335505	5.654409
9	0.80	4.130817	0.339736	5.669208
10	0.90	4.139806	0.343969	5.681543
11	1.00	4.147007	0.348202	5.691426
12	1.10	4.152471	0.352429	5.698924
13	1.20	4.156213	0.356651	5.704061
14	1.30	4.158244	0.360864	5.706848
15	1.40	4.158599	0.365063	5.707335
16	1.50	4.157314	0.369249	5.705572
17	1.60	4.154387	0.373416	5.701555
18	1.70	4.149846	0.377565	5.695323
19	1.80	4.143713	0.381693	5.686906
20	1.90	4.136028	0.385796	5.676359
21	2.00	4.126792	0.389876	5.663683
22	3.00	3.953794	0.428945	5.426256
23	4.00	3.647243	0.464082	5.005542
24	5.00	3.224684	0.494513	4.425613
25	6.00	2.703265	0.519774	3.710009
26	7.00	2.100711	0.539597	2.883053
27	8.00	1.435872	0.553831	1.970616
28	9.00	0.728641	0.562396	1.000000
29	10.00	0.000000	-0.847966	0.000000

WEDGE ANGLE = 10.00 SOURCE ANGLE = 2.50
SOURCE DISTANCE=0.75 RECEIVER DISTANCE= 0.28 SHORE DISTANCE= 0.00
RHO1/RHO2= 0.80 C1/C2= 1.10 ALPHA/K2= 0.0001
K1X = 19.44

REC.POS	REC.ANGLE	PRES.AMPLITUDE	PHASE ANGLE	NORM.PRESS
1	0.00	0.642356	-0.271448	9.791314
2	0.10	0.636151	-0.270972	9.696724
3	0.20	0.629941	-0.270501	9.602075
4	0.30	0.623727	-0.270035	9.507351
5	0.40	0.617507	-0.269567	9.412549
6	0.50	0.611286	-0.269111	9.317716
7	0.60	0.605059	-0.268658	9.222797
8	0.70	0.598825	-0.268203	9.127778
9	0.80	0.592588	-0.267760	9.032702
10	0.90	0.586344	-0.267313	8.937539
11	1.00	0.580099	-0.266874	8.842341
12	1.10	0.573846	-0.266441	8.747032
13	1.20	0.567591	-0.266014	8.651687
14	1.30	0.561331	-0.265585	8.556263
15	1.40	0.555062	-0.265165	8.460711
16	1.50	0.548791	-0.264745	8.365122
17	1.60	0.542518	-0.264339	8.269497
18	1.70	0.536235	-0.263923	8.173734
19	1.80	0.529949	-0.263521	8.077916
20	1.90	0.523657	-0.263120	7.982002
21	2.00	0.517360	-0.262721	7.886027
22	3.00	0.454118	-0.259016	6.922033
23	4.00	0.390374	-0.255795	5.950404
24	5.00	0.326155	-0.253081	4.971522
25	6.00	0.261508	-0.250935	3.986116
26	7.00	0.196416	-0.247807	2.993931
27	8.00	0.131108	-0.246445	1.998455
28	9.00	0.065605	-0.245626	1.000000
29	10.00	0.000001	-0.026186	0.000009

APPENDIX D
TABLES

TABLE 1

RECEIVER DISTANCE AT THE FIRST TRANSITION POINT, FOR CONSTANT $\rho_1/\rho_2 = 0.80$, $c_1/c_2 = 1.10$

$\beta = 6^{o}$, $K_1X = 32.61$

	$R_1 = 1.10$	$R_1 = 1.20$	$R_1 = 1.30$	$R_1 = 1.40$	$R_1 = 1.50$
$\gamma = \beta/4$	5.2	5.0	5.9	7.3	9.8
$\gamma = \beta/2$	5.2	4.7	5.7	6.8	9.9
$\gamma = 3\beta/4$	4.0	4.5	5.4	7.0	10.5

$\beta = 10^{o}$, $K_1X = 19.44$

	$R_1 = 0.80$	$R_1 = 0.90$	$R_1 = 1.00$	$R_1 = 1.10$	$R_1 = 1.20$
$\gamma = \beta/4$	17.5	24.0	33.0	52.0	72.0
$\gamma = \beta/2$	12.5	17.0	24.0	42.0	60.0
$\gamma = 3\beta/4$	10.6	17.0	22.0	40.0	58.0

$\beta = 15^{o}$, $K_1X = 12.79$

	$R_1 = 1.30$	$R_1 = 1.40$	$R_1 = 1.50$	$R_1 = 1.60$	$R_1 = 1.70$
$\gamma = \beta/4$	8.1	8.2	8.7	9.8	11.4
$\gamma = \beta/2$	6.9	7.0	7.8	8.9	10.9
$\gamma = 3\beta/4$	9.8	12.0	15.0	19.0	29.0

TABLE 2

RECEIVER DISTANCE AT THE FIRST TRANSITION POINT, FOR CONSTANT $\rho_1/\rho_2 = 0.80$, $c_1/c_2 = 1.20$

$\beta = 6^o$, $K_1X = 22.53$

	$R_1 = 1.30$	$R_1 = 1.40$	$R_1 = 1.50$	$R_1 = 1.60$	$R_1 = 1.70$
$\gamma = \beta/4$	3.37	3.6	3.92	4.4	4.96
$\gamma = \beta/2$	3.155	3.42	3.78	4.36	4.96
$\gamma = 3\beta/4$	3.07	3.34	3.74	4.2	5.1

$\beta = 10^o$, $K_1X = 13.43$

	$R_1 = 0.80$	$R_1 = 0.90$	$R_1 = 1.00$	$R_1 = 1.10$	$R_1 = 1.20$
$\gamma = \beta/4$	6.1	11.3	18.0	40.0	60.0
$\gamma = \beta/2$	6.5	8.2	14.5	25.0	40.0
$\gamma = 3\beta/4$	5.05	5.45	12.0	18.0	30.0

$\beta = 15^o$, $K_1X = 8.84$

	$R_1 = 0.80$	$R_1 = 0.90$	$R_1 = 1.00$	$R_1 = 1.10$	$R_1 = 1.20$
$\gamma = \beta/4$	36.0	40.0	52.0	60.0	64.0
$\gamma = \beta/2$	24.0	26.0	32.0	46.0	54.0
$\gamma = 3\beta/4$	19.50	23.0	28.0	38.0	58.0

TABLE 3

RECEIVER DISTANCE AT THE FIRST TRANSITION POINT, FOR CONSTANT $\rho_1/\rho_2 = 0.90$, $c_1/c_2 = 1.10$

$\beta = 6^o$, $K_1X = 32.61$

	$R_1 = 1.10$	$R_1 = 1.20$	$R_1 = 1.30$	$R_1 = 1.40$	$R_1 = 1.50$
$\gamma = \beta/4$	3.66	4.1	4.9	6.2	11.0
$\gamma = \beta/2$	3.35	3.9	4.7	7.0	no
$\gamma = 3\beta/4$	3.24	3.76	4.75	7.3	9.8

$\beta = 10^o$, $K_1X = 19.44$

	$R_1 = 1.30$	$R_1 = 1.40$	$R_1 = 1.50$	$R_1 = 1.60$	$R_1 = 1.70$
$\gamma = \beta/4$	9.8	11.0	14.0	40.0	60.0
$\gamma = \beta/2$	7.6	8.6	11.0	19.0	40.0
$\gamma = 3\beta/4$	6.7	7.6	10.0	21.0	45.0

APPENDIX E

GRAPHS OF R_1 VERSUS R_2 AT THE FIRST TRANSITION POINT

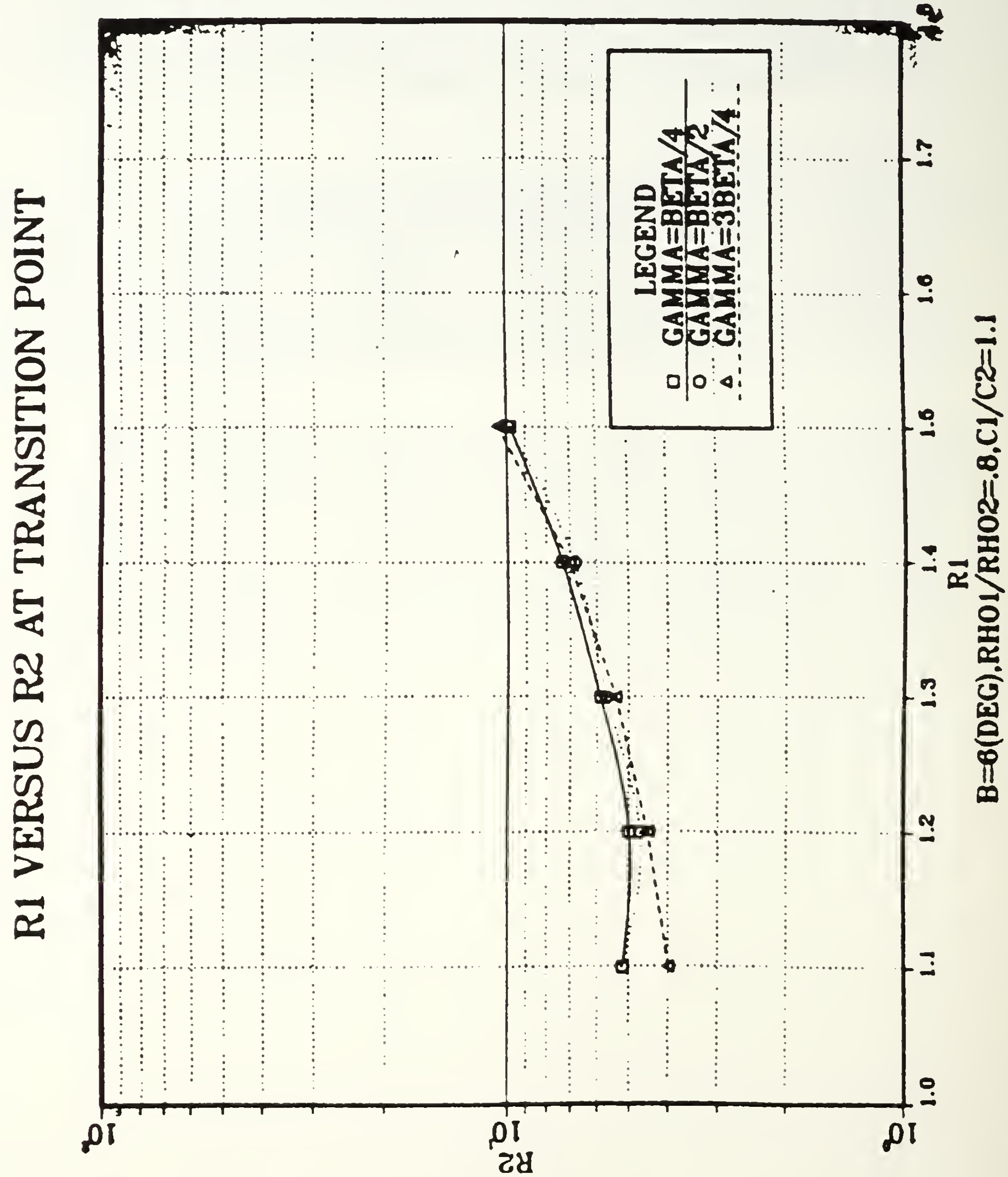

Figure E.1 R_1 vs R_2 at the first trans.points, for $\beta = 6^{\circ}$, $\rho_1/\rho_2 = 0.80$, $c_1/c_2 = 1.10$.

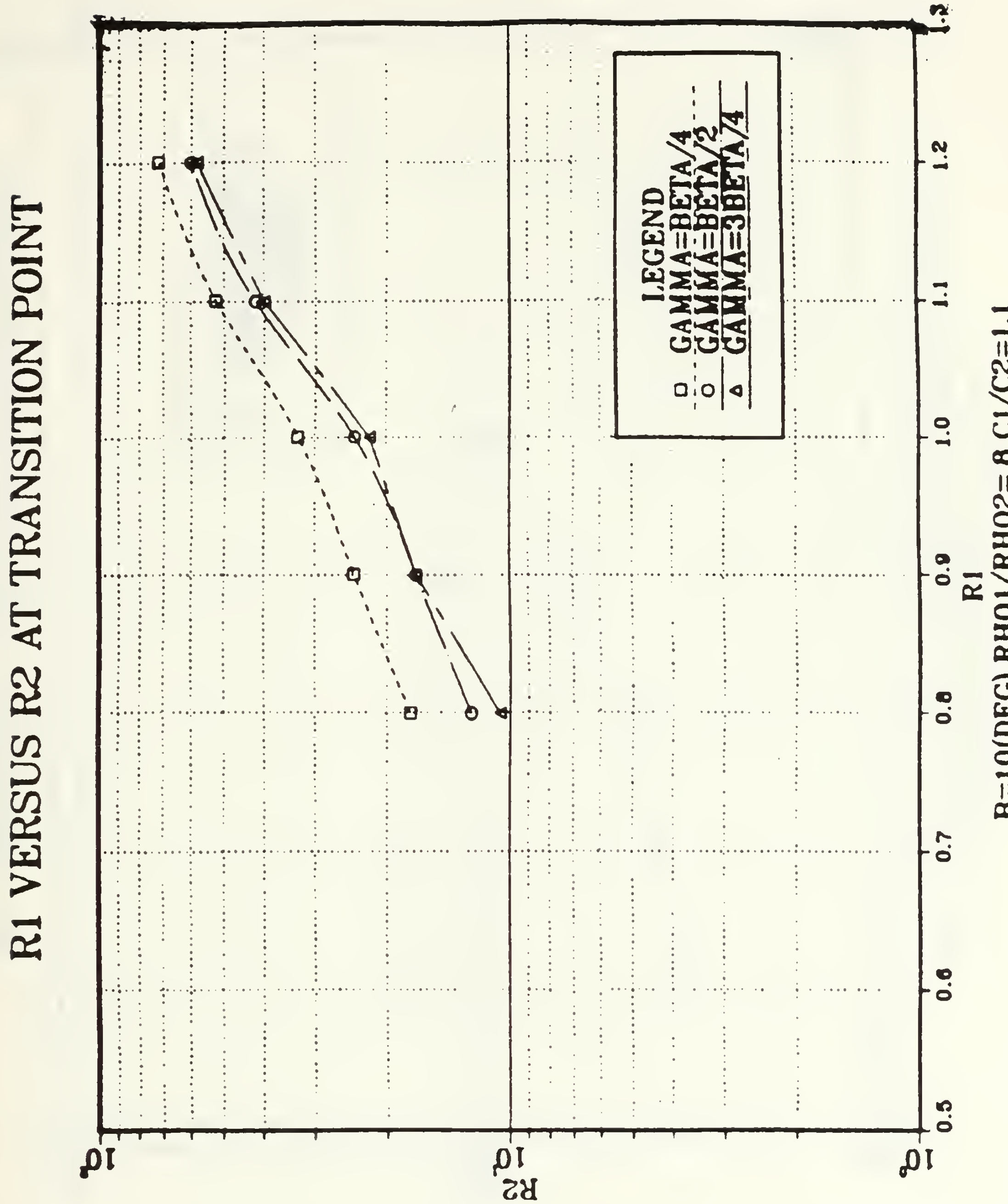

Figure E.2 R_1 vs R_2 at the first trans. points, for $\beta = 10^{\circ}$, $\rho_1/\rho_2 = 0.80$, $c_1/c_2 = 1.10$.

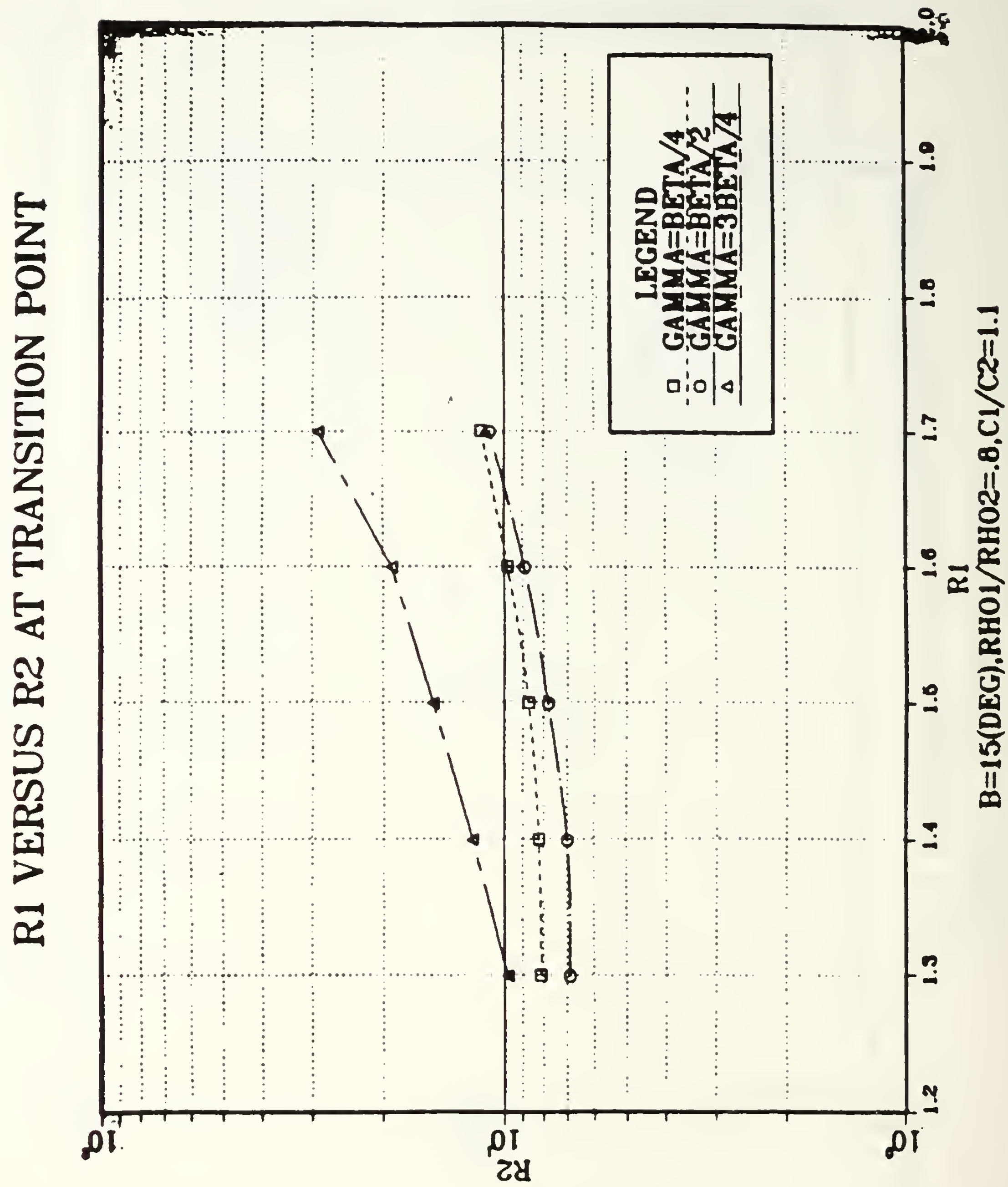

Figure E.3 R_1 vs R_2 at the first trans. points, for $\beta = 15^o$, $\rho_1/\rho_2 = 0.80$, $c_1/c_2 = 1.10$.

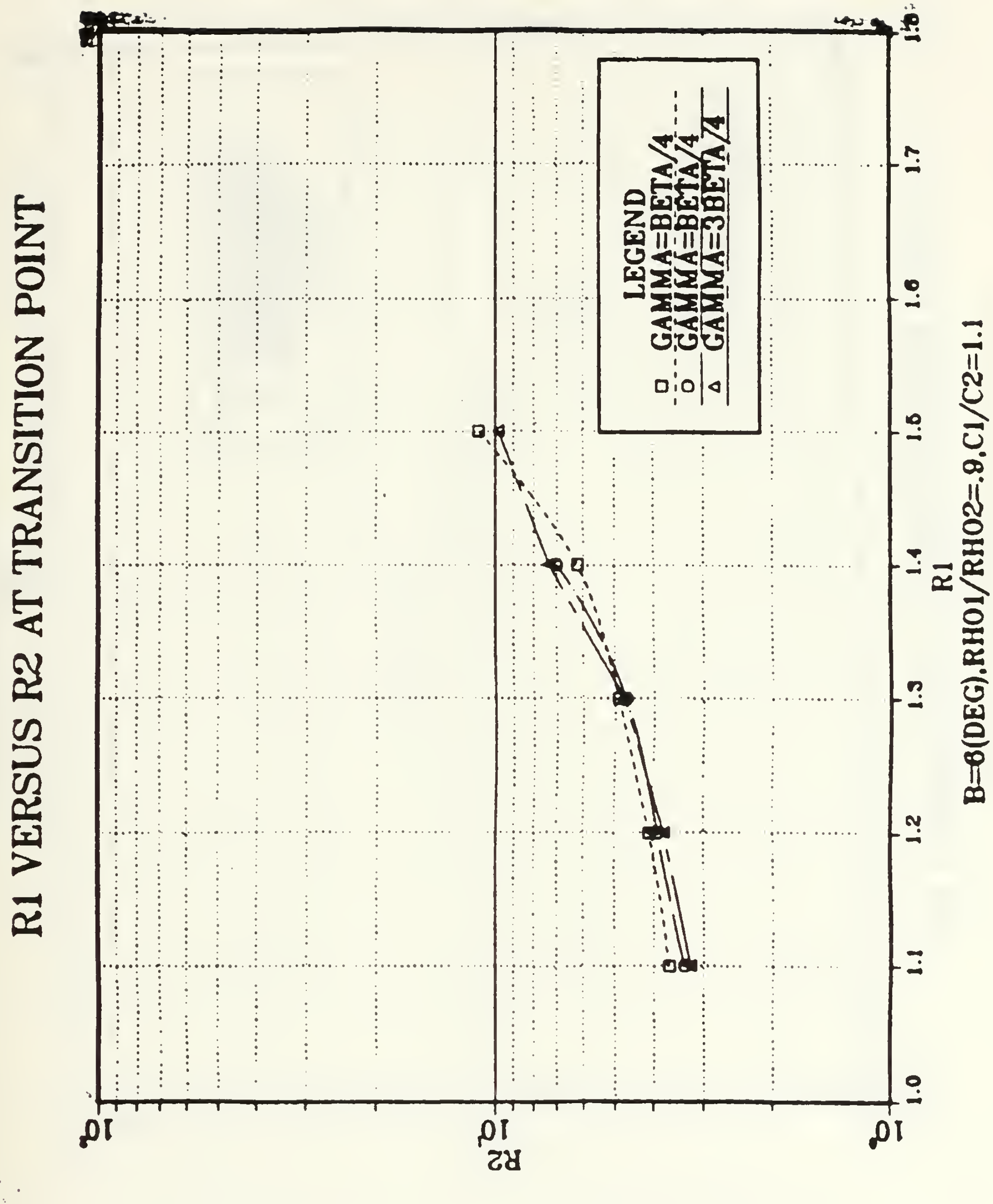

Figure E.4 R_1 vs R_2 at the first trans. points, for $\beta = 6^o$, $\rho_1/\rho_2 = 0.80$, $c_1/c_2 = 1.20$.

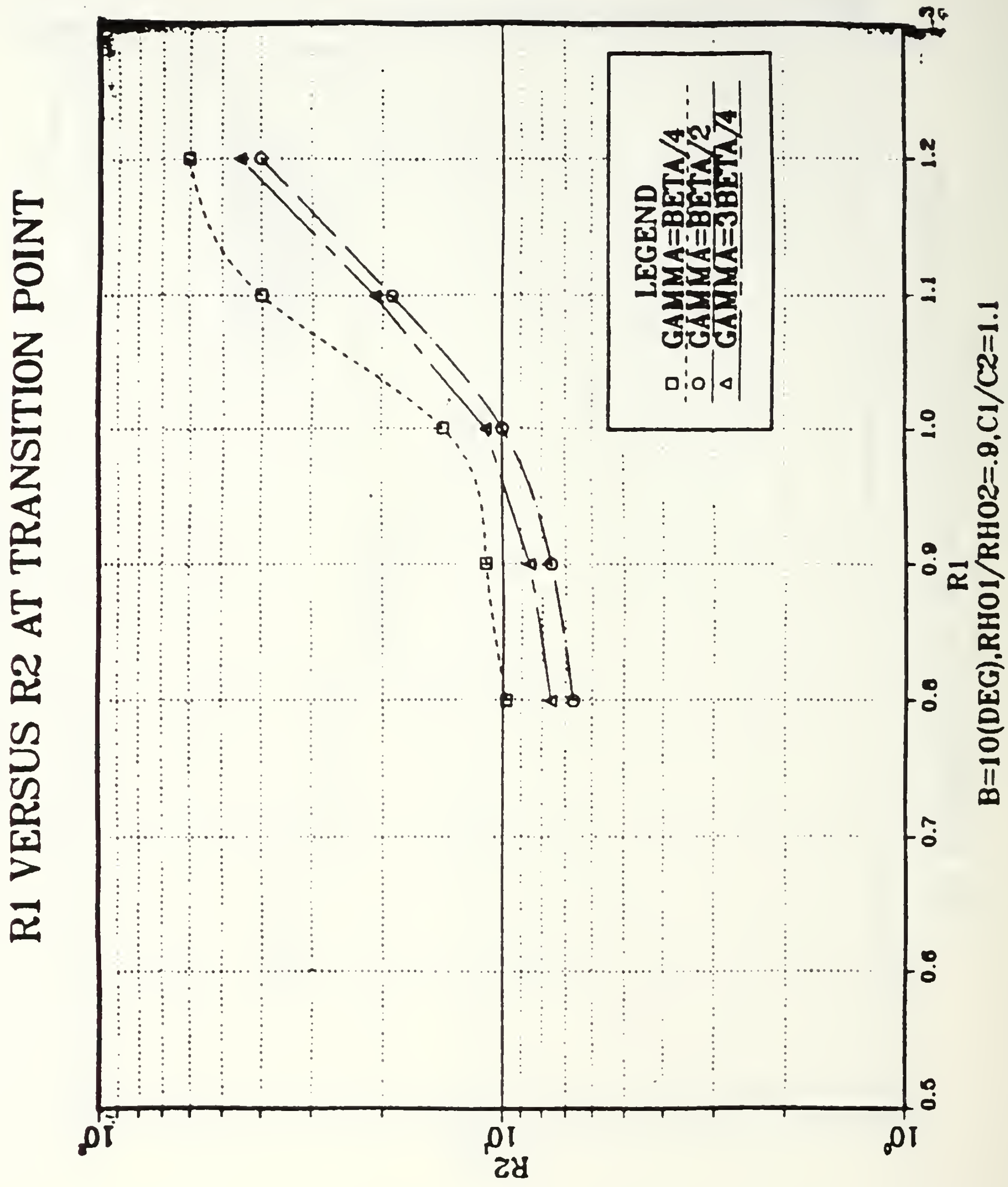

Figure E.5 R_1 vs R_2 at the first trans. points, for $\beta = 10^{o}$, $\rho_1/\rho_2 = 0.80$, $c_1/c_2 = 1.20$.

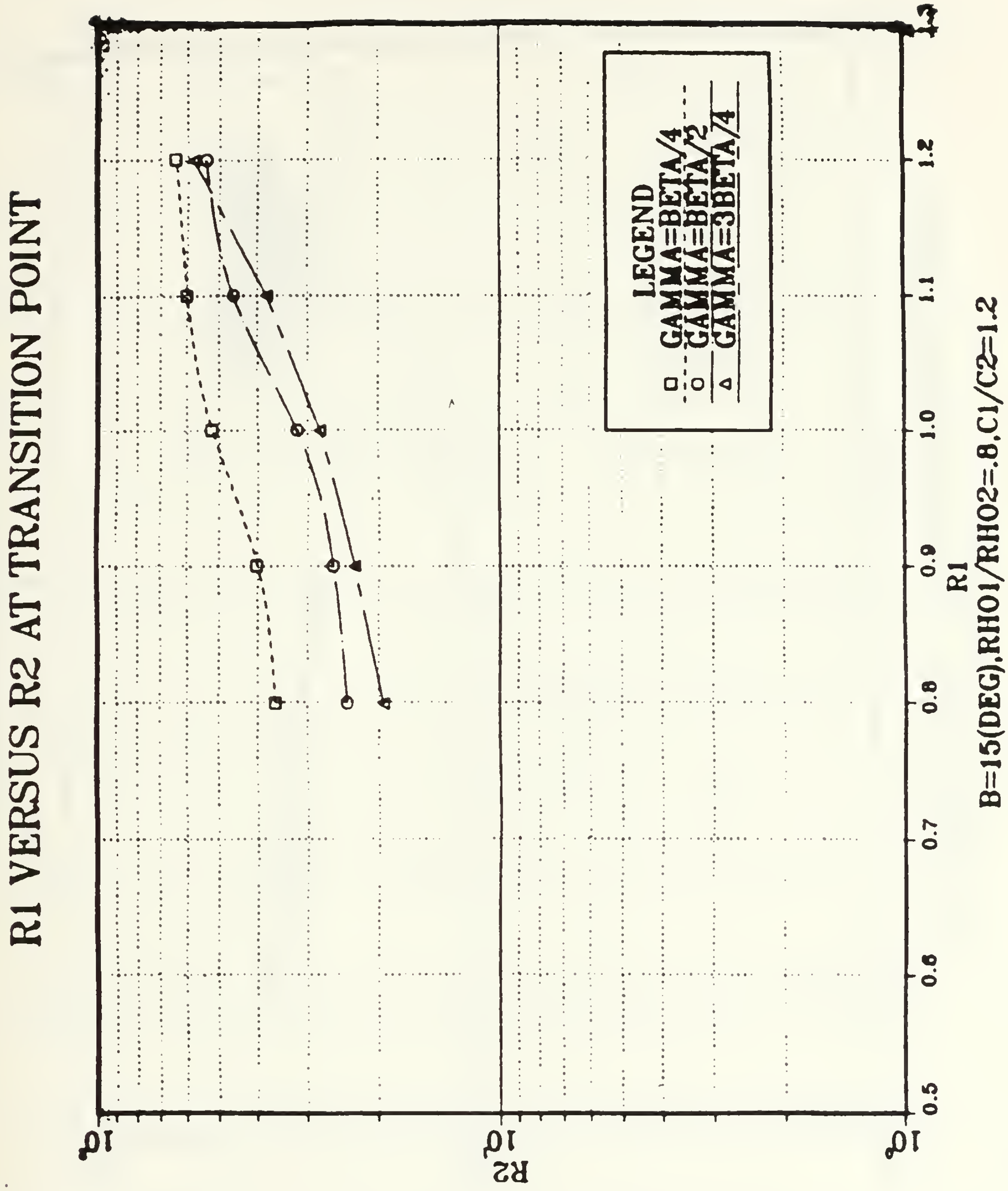

Figure E.6 R_1 vs R_2 at the first trans. points, for $\beta = 15^{\circ}$, $\rho_1/\rho_2 = 0.80$, $c_1/c_2 = 1.20$.

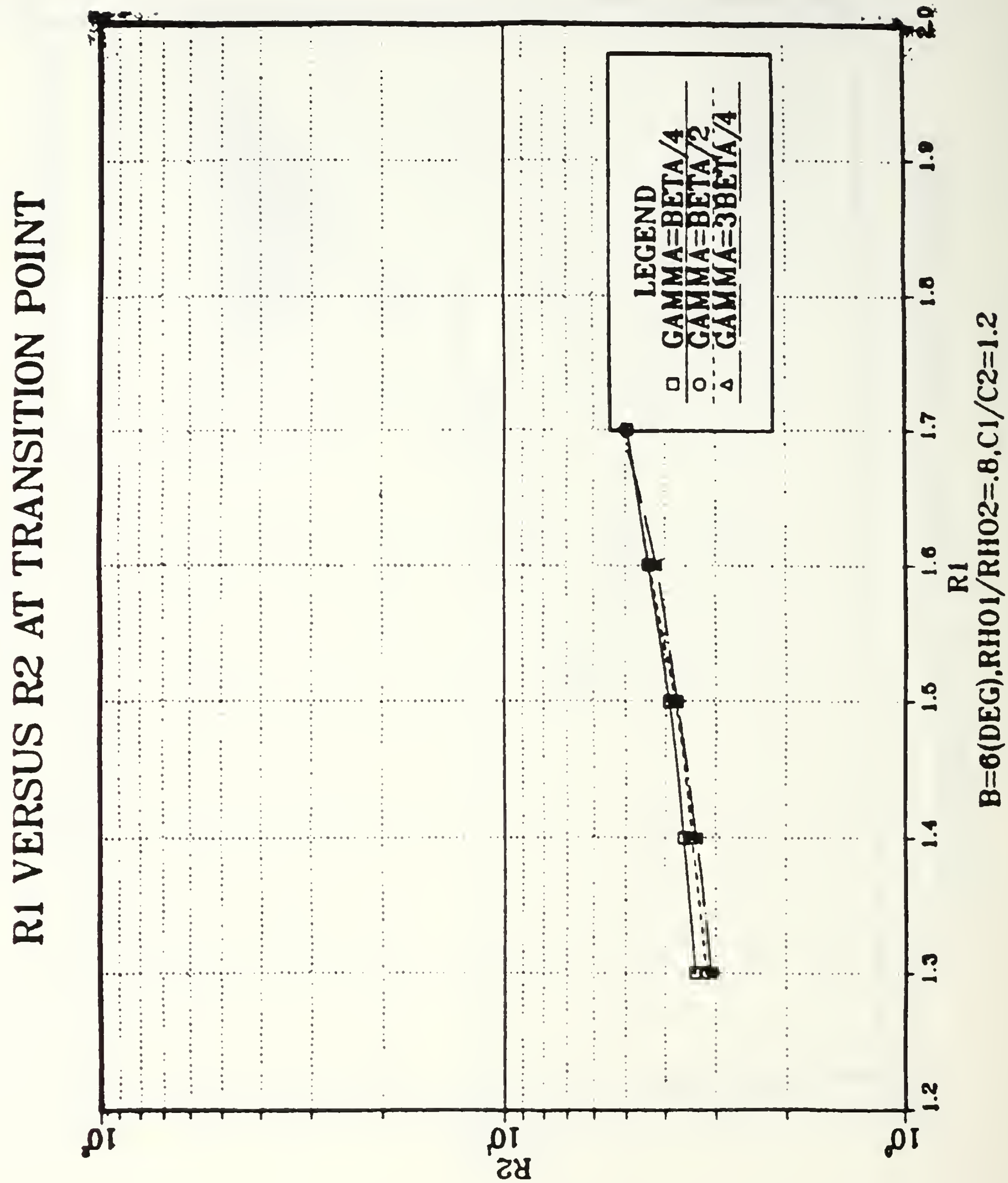

Figure E.7 R_1 vs R_2 at the first trans. points, for $\beta = 6^{o}$, $\rho_1/\rho_2 = 0.90$, $c_1/c_2 = 1.10$.

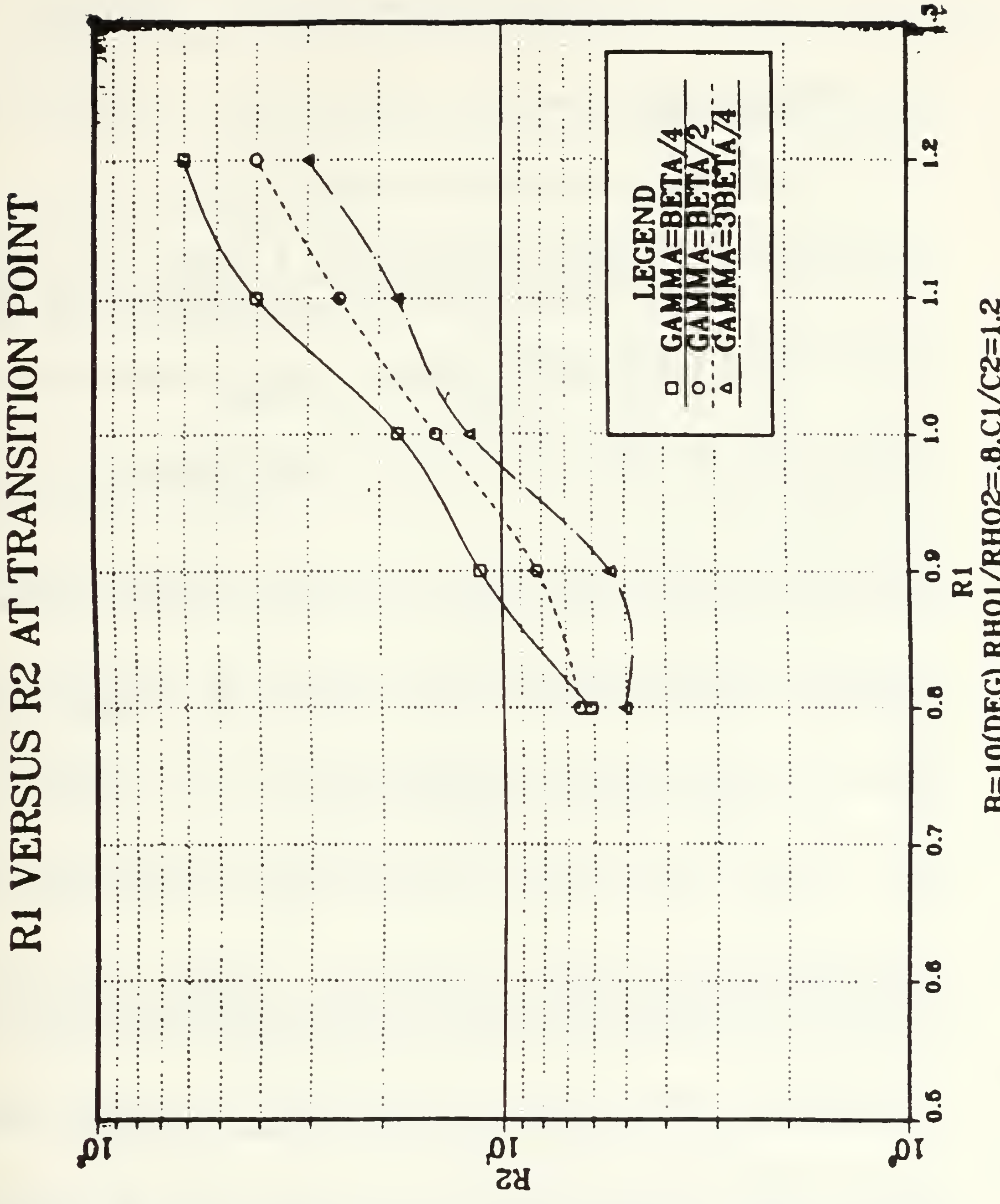

Figure E.8 R_1 vs R_2 at the first trans. points, for $\beta = 10^o$, $\rho_1/\rho_2 = 0.90$, $c_1/c_2 = 1.10$.

LIST OF REFERENCES

1. C. L. Pekeris. *Theory of Propagation of Explosive Sound in Shallow Water*, Geol. Soc. Am. Mem. 27(1948).

2. L. Brekovskikh, *Waves in Layered Media*, Academic Press, New York, 1960.

3. R. D. Graves, Anton Nagl, H. Uberall and G. L. Zauer, *Range Dependent Normal Modes in Underwater Sound Propagation: Application to the Wedge-Shaped Ocean*, Journal of Acoustical Society of America 58(6), December 1975.

4. J. M. Arnold and L. B. Felsen *Rays and Local Modes in a Wedge-shaped ocean*, Journal of Acoustical Society of America 73(4), April 1983.

5. A. Kamel and L. B. Felsen *Spectral Theory of Sound Propagation in an Ocean Channel with Weakly Sloping Bottom*, Journal of Acoustical Society of America, 73(4), April 1983.

6. Allan D. Pierce, *Guided Mode Disappearance During Upslope Propagation in Variable Depth Shallow Water Overlying a fluid bottom*, Journal of Acoustical Society of America, 72(2), August 1982.

7. Suzanne T. McDaniel, *Parabolic Approximations for Underwater Sound Propagation*. Journal of Acoustical Society of America, 58(6), December 1975.

8. Ding Lee and John S. Papadakis, *Numerical Solutions of the Parabolic Wave Equation: An OrdinaryDifferential-Equation Approach*,

9. F. B. Jensen and W. A. Kuperman, *Sound Propagation in a Wedge-Shaped Ocean With a Penetrable Bottom*, Journal of Acoustical Society of America, 67(5), May 1980.

10. A. B. Coppens, J. V. Sanders, M. Kawamura, I. Ioannou, *Two Computer Programs for the Evaluation of the Acoustic Pressure Amplitude and Phase of the Bottom of a Wedge-Shaped, Fluid Layer Overlying a Fast Fluid Half-Space*, Naval Postgraduate School, Monterey, CA 93943, December 1978.

11. Chil Ki Baek *The Acoustic Pressure in a Wedge Shaped Water Layer Overlying a Fast Fluid Bottom*, Naval Postgraduate School, M.S.Thesis, March 1984.

12. Patrick S. LeSesne *Development of Computer Programs Using the Method of Images to Predict the Sound Field in a Wedge Overlying a Fast Fluid and Comparison with Laboratory Experiments*, Naval Postgraduate School, M.S.Thesis, December 1984.

13. A. B. Coppens *A Personal Commmunication* Naval Postgraduate School, Monterey, CA 93943, July 1986.

14. Ioannis Iouannou and Masami Kawamura *Pressure on the Interface between a Converging Fluid Wedge and a Fast Fluid Bottom*, Naval Postgraduate School, M.S. Thesis, December 1978.

15. Kinsler, Frey, Coppens and Sanders, *Fundamentals of Acoustics*, John Wiley & Sons, third edition, 1982

INITIAL DISTRIBUTION LIST

		No. of Copies
1.	Defense Technical Information Center Cameron Station Alexandria, Virginia 22304-6145	2
2.	Library, Code 0142 Naval Postgraduate School Monterey, California 93943-5002	2
3.	Department Library, Code 61 Department of Physics & Chemistry Naval Postgraduate School Monterey, California 93943-5000	1
4.	Dr. A. B. Coppens, Code 61Cz Department of Physics Naval Postgraduate School Monterey, California 93943-5000	2
5.	Dr. J. V. Sanders, Code 33A Weapons System Academic Associate Naval Postgraduate School Monterey, California 93943-5000	2
6.	CDR Chil Ki Baek SMA 1646, Naval Postgraduate School Monterey, California 93943-5000	1
7.	CDR Carolus Kaswandi Dinas Penelitian Dan Pengembangan TNI-AL Jl.Jati, Pangkalan Jati Jakarta Selatan, Indonesia	3
8.	Perpustakaan Pusat Markas Besar TNI-AL Cilangkap Jakarta Timur, Indonesia	1
9.	Pusat Dokumentasi Ilmiah Nasional JL. Gatot Subroto Jakarta Selatan, Indonesia	2
10.	Pusat Pendidikan Ilmu Dan Teknologi TNI-AL Bumi Morokrembangan Surabaya, Indonesia	2

11. Dinas Penelitian Dan Pengembangan TNI-AL 1
Jl. Jati, Pangkalan Jati
Jakarta, Indonesia

12. Dr. James Andrews 1
NSTL Station
Bay St. Louis, Mississippi 39529

13. Dr. Michael McKissic 1
Chief of Naval Research
800 N. Quincy Street
Arlington, Virginia 22217

14. Mr. Gene Brown 1
NAVOCEANO, Code 7300
NSTL Station
Bay St. Louis, Mississippi 39522

15. Dr. Robert Martin 1
NORDA 110A
NSTL Station
Bay St. Louis, Mississippi 39466

16. Asst. Professor C. Dunlap, Code 68Du 1
Department of Oceanography
Naval Postgraduate School
Monterey, California 93943-5000

17. Marie B. Hashimoto 1
Department of Aeronautics, Code 67
Naval Postgraduate School
Monterey, California 93943-5000

Thesis
K1451
c.1

Kaswandi
A computerized investigation using the method of images to predict the sound field in a fluid wedge overlying a slow fluid half-space.